IDO-16430

Progress Reports
(TID-4500, 13th Ed. Suppl.)

QUARTERLY PROGRESS REPORT FOR MTR-ETR TECHNICAL BRANCHES
Third Quarter - 1957

Edited by K. A. McCollom

December 16, 1957

AEC RESEARCH AND DEVELOPMENT REPORT

PHILLIPS PETROLEUM CO.
ATOMIC ENERGY DIVISION
(UNDER CONTRACT NO. AT (10-1)-205)
IDAHO OPERATIONS OFFICE
U. S. ATOMIC ENERGY COMMISSION

DISCLAIMER

PRICE $2.00

Available from the
Office of Technical Services
U. S. Department of Commerce
Washington 25, D. C.

LEGAL NOTICE

PAGES 1 to 2

WERE INTENTIONALLY

LEFT BLANK

TABLE OF CONTENTS

TABLE OF CONTENTS - CONT'D.

LIST OF FIGURES

LIST OF FIGURES - CONT'D.

QUARTERLY PROGRESS REPORT FOR MTR-ETR TECHNICAL BRANCHES
Third Quarter - 1957

Edited by - K. A. McCollom

Work Directed by*- D. R. deBoisblanc, Director, Reactor Physics and Engineering Branch
W. B. Lewis, Director, Theoretical Physics and Applied Mathematics Branch
J. E. Evans, Director, Nuclear Physics Branch

I. SUMMARY

MTR-ETR Technical Assistance - The Engineering Test Reactor Critical Facility fuel loading was increased from a 49 element core to a 59 element core to give an excess reactivity of 11% in $\Delta k/k$. Statistical weights and thermal flux measurements have been made throughout the core. A means of estimating variation in boron content in ETR fuel elements by comparing a standard fuel element with a dummy element and an element containing only fuel showed the average boron content per fuel element to be 0.65 grams more than the specified 1.6 grams. The equivalent total curie value of MTR fuel elements and the curie content of several specific isotopes has been worked out. By operating 228 hours in addition to the regular day shifts, the Machine Computational Facility (IBM 650) achieved 675 hours of production time this quarter.

MTR-ETR Development - Four experimental shim rod magnets have already operated successfully without failure for longer than the average life of existing MTR shim rod magnets. The lower original cost, the replaceable coil feature, and the negligible maintenance for the experimental magnet should drastically reduce the maintenance attention presently required in the MTR. Refinements have been made on the calculations of MTR fuel charge and Xenon override. Prediction of MTR charge life has been made using ingrowth of Xe-135 after a power reduction with an improved accuracy compared to previous methods. Methods of measuring both boron and fuel contained in ETR elements by chemical and non-destructive techniques are being evaluated. Hydraulic tests have been made on four modifications of the ETR fuel element design. A study of the effects of varying parameters and changing design of fuel elements has been conducted. Pre-irradiation metallographic examination of representative fuel sample plates has been completed. Preliminary planning has been completed on proposed experiments to study the reaction of molten metals with water in the reactor.

Reactor Physics and Engineering - A method of obtaining the lethargy dependence of the flux, $\Phi(u)$, to obtain the fast group constants for group diffusion theory calculations has been programmed for the IBM-650.

---

* With contributions from the Operations Evaluation Branch.

The revised result of the yield of I-135 was 4.1 ± 0.6% in the fission of plutonium. A thorium slug irradiated for a year in the MTR was sectioned and analyzed to obtain the distribution of uranium within the slug. No significant angular dependence about the axis of the slug was observed.

Nuclear Physics - The major emphasis of the cross section program has been on understanding the fission process in U-233. The 1024 channel time-of-flight analyzer with an automatic detector delay-correction system has completely replaced the original 100 channel analyzer. Total cross section curves are given on Pu-240, Sm, Gd, Ca, Sr, and Li-7. The HG-6 beam hole plug for the inelastic-scattering-of-slow-neutrons program has been installed in the MTR, and radiation and temperature measurements have been made at an operating power of 40Mw. Initial development is under way on a 1024 channel time-of-flight analyzer for the scattering data accumulation. In nuclear chemistry the Mo^{99}/Ag^{113} saturation activity ratios of the fission of U-233 with thermal and 1.8 ev neutrons were compared with the latter result appearing larger by about 15 per cent. Several second order capture measurements are being investigated. In the decay schemes program, the machine calculated detection efficiencies of sodium iodide scintillation crystals are being checked experimentally. The decay schemes of Bi-205 and La-142 are being investigated.

II. MTR-ETR TECHNICAL ASSISTANCE

A. Engineering Test Reactor Critical Facility (E. E. Burdick)

1. Reactor Measurements (B. L. Hanson, J. W. Henscheid, D. L. Parry, T. K. DeBoer)

The initial full-core loading in the ETR Critical contained 49 fuel elements with a measured excess reactivity of 1.5% in $\Delta k/k$.(1) This loading was increased to 59 elements (by eliminating several experimental positions) to give an excess reactivity of 11% in $\Delta k/k$. An average total flux of 2.9×10^8 neut./cm^2 sec in the 49 element core corresponds to approximately 200 watts. In the 59 element core a total average flux of 2.9×10^8 neut./ cm^2 sec corresponds to approximately 220 watts.

The "start-up" core for the ETR using 59 elements was loaded in the ETR Critical prior to being used in the ETR start-up. The difference in excess reactivity compared to the 59 elements used in the original loading of the ETR Critical was -0.47% in $\Delta k/k$.

Statistical weights have been measured in many representative positions throughout the core with 36 inch boron impregnated tapes and vary from negligible to 0.2% in $\Delta k/k$ per gram of boron.

2. Fuel Element Measurements (D. L. Parry)

As a means of estimating the variation in boron content in the fuel elements, the reactivity differences between 10 fuel elements picked at random were measured in a given position in the ETR Critical. The percent standard deviation was found to be 2.6%. Each of the fuel elements was compared to a dummy element (one containing no fuel or boron) and a fuel element containing fuel but no boron. Since the statistical weight, ω, of boron was known, the amount of boron per fuel element could then be computed with the following relationships:

$$\rho_{\text{fuel}} - \left(\rho_{\text{fuel}} + \rho_{\text{boron}}\right) = \rho_{\text{boron}} \qquad \text{II-1}$$

$$\frac{\rho_{\text{boron}}}{\omega_{\text{boron}}} = \text{boron content in grams} \qquad \text{II-2}$$

ρ is the reactivity per gram of the fuel and boron respectively. The average boron content per fuel element computed in this manner was found to be about 0.65 grams more than that reported by Babcock and Wilcox (nominally 1.6 grams). This estimate neglects self shielding.

Investigations of modifications of the present ETR fuel element to increase its structural rigidity led to several experiments in the ETR Critical Facility. Changing the metal-to-water ratio of the ETR elements from the present 0.64 to 0.84 resulted in a net decrease in the excess reactivity of 1.66% in $\Delta k/k$.

Changing the boron from the fuel plates to either (1) the side plates or (2) a simulated center plate, showed no significant depression in a horizontal midplane flux traverse through the fuel element.

3. Control Rod Worths (J. W. Henscheid)

Values for the net worths of the ETR Critical Facility control rods were found to vary considerably due to perturbation effects caused by changing nearby control rods from poison to fuel and vice versa. However, the averages of values obtained throughout the core were as follows:

Gray rod (nickel)	1.0% in $\Delta k/k$
Black rod (cadmium - aluminum)	1.4% in $\Delta k/k$
Black rod (boron - stainless steel)	1.6% in $\Delta k/k$

Of the two types of black rods mentioned, the cadmium - aluminum rods are used in the ETR Critical Facility since the boron - stainless steel rods were not immediately available.

Of specific interest is the calibration of the motor driven gray (shim) rod in the ETR Critical Facility. To check the validity of calibration methods this rod was evaluated by three different methods with the following results:

Period Measurements (local poison additions)	1.00% $\Delta k/k$
Period Measurements (distributed poison)	.90% $\Delta k/k$
Distributed poison $\left(\frac{\Delta \Sigma}{\Sigma \text{ pile}}\right)$	.98% $\Delta k/k$

Since the regulating rod drive is not yet operable the regulating rod was not calibrated, but its net worth was measured to be 0.01% in $\Delta k/k$ in its present position. It is planned to change the regulating rod to another position, however, in order to increase its worth to approximately 0.3% in $\Delta k/k$.

4. Thermal Flux Measurement (P. W. Healy)

Flux measurements have been made in the ETR Critical Facility to compare with a comparable core in the ETR. The flux measurements from the ETR Critical Facility will simplify the determination of hot spots in the ETR and will provide the Theoretical Physics Section with data for calculations for the ETR.

The most extensive flux mapping was made on the 59 element core shown in Figure 1 since this is the core which will be used for most of the Start-up tests in the ETR. The position of the shim rods, whether "IN" or "OUT" is indicated in the figure. The flux measurements were made either with 5 mil circular gold foils 3/16 inches in diameter, or with 40 mil gold wire usually 3 or 5 inches in length. The wires were used principally to determine the cadmium ratios, and when so used were covered with close fitting cadmium sleeves on the lower half of the 3" wires and on the center section of the 5" wires. The foils or wires were either secured to the side of the fuel elements with short sections of black plastic electricians' tape, or they were fastened to plastic wands or aluminum stringers and inserted in the fuel elements and aluminum filler pieces.

ETRC CORE

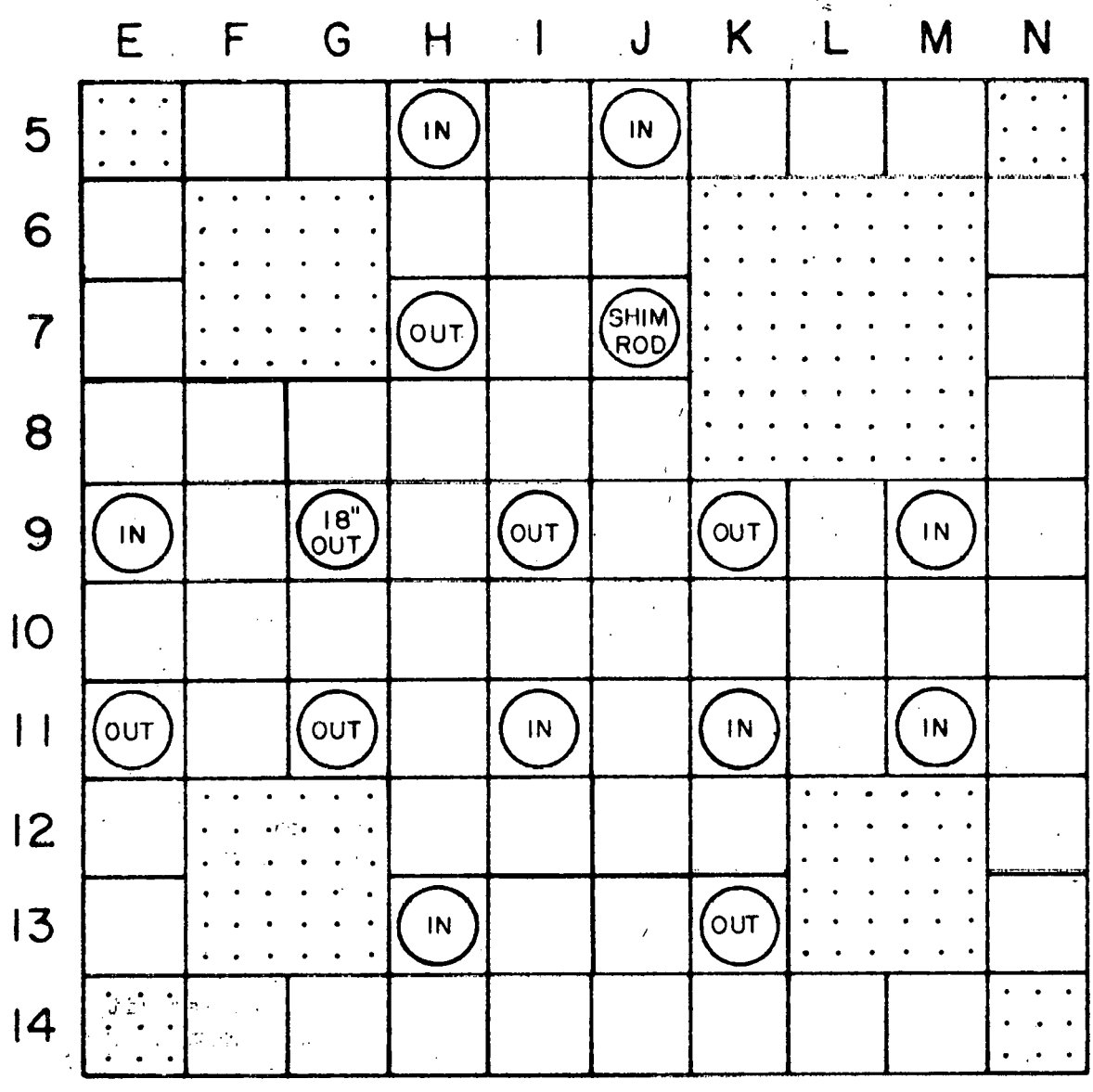

ALUMINUM FILLER PIECES

CONTROL RODS

FUEL ELEMENTS
FUEL ELEMENTS ARE APPROXIMATELY 3" SQUARE

FLUX MAPPING CONFIGURATION

FIGURE 1

Figure 2 gives the values of the Cd ratios used in determining the thermal flux map. The underscored values are experimentally determined and the other values are interpolations. Figure 3 gives values proportional to the thermal flux as determined from the total count of the gold foils or wires and the Cd ratios. Figure 4 is a rough thermal flux map based on these data. Figure 5 gives vertical flux traverses for selected positions in the core.

B. Curie Value of Spent MTR Fuel Elements (W. C. Francis, E. H. Porter)

1. Total Equivalent Curies

Requests for shipping purposes and from users of spent MTR fuel elements have indicated the need for assigning some curie value to these elements. Normally the gamma decay dose rate at a specified distance from the spent fuel is expressed in roentgens per hour. Confusion arises in trying to assign a curie value since more than 100 nuclides are known to emit gammas during the decay of U-235 fission products. These vary widely in half life and energy so that the energy spectrum changes throughout the cooling period. It is usual to assume that each disintegration in the fission products results in the liberation of one gamma photon. Each disintegration of Co-60 on the other hand yields two gamma photons of 1.17 and 1.33 Mev energy. A curie value based on the total disintegrations of all fission products will be quite different, therefore, from one related directly to a Co-60 equivalent curie value. Although several local sources had reported curie values for the spent MTR fuel elements, they were based on different assumptions. A series of decay curves have, therefore, been prepared for use by the MTR Operations Branch summarizing the past work and applying suitable corrections for the present 40 Mw operation of the MTR. Table I shows a sample of the results of this work. Column A is in the usual r/hr terms, and Column B is based on the work in IDO-16247(2) which sums the disintegrations per second for various energy groups. Column C is based on measured data of C. H. Hogg using a standard 168-curie Co-60 source.

TABLE I

TYPICAL SPENT MTR FUEL ELEMENT DECAY RATE FOR A BURNUP OF 28.5% AT 40 MW OPERATION

Decay Time After Shutdown (days)	A r/hr (through 3" water)	B Total Curies	C** Co-60 Equiv. Curies
10	18.0×10^5	$16. \times 10^4$	5.2×10^4
50	4.2×10^5	3.6×10^4	1.1×10^4
100	1.9×10^5	1.3×10^4	$.5 \times 10^4$
200	$.8 \times 10^5$	$.35 \times 10^4$	$.2 \times 10^4$
300		$.14 \times 10^4$	

** Defined as that amount of Co-60 distributed over the same volume as the fuel element, which would produce the same gamma dosage rate as the fuel element.

ETRC CORE

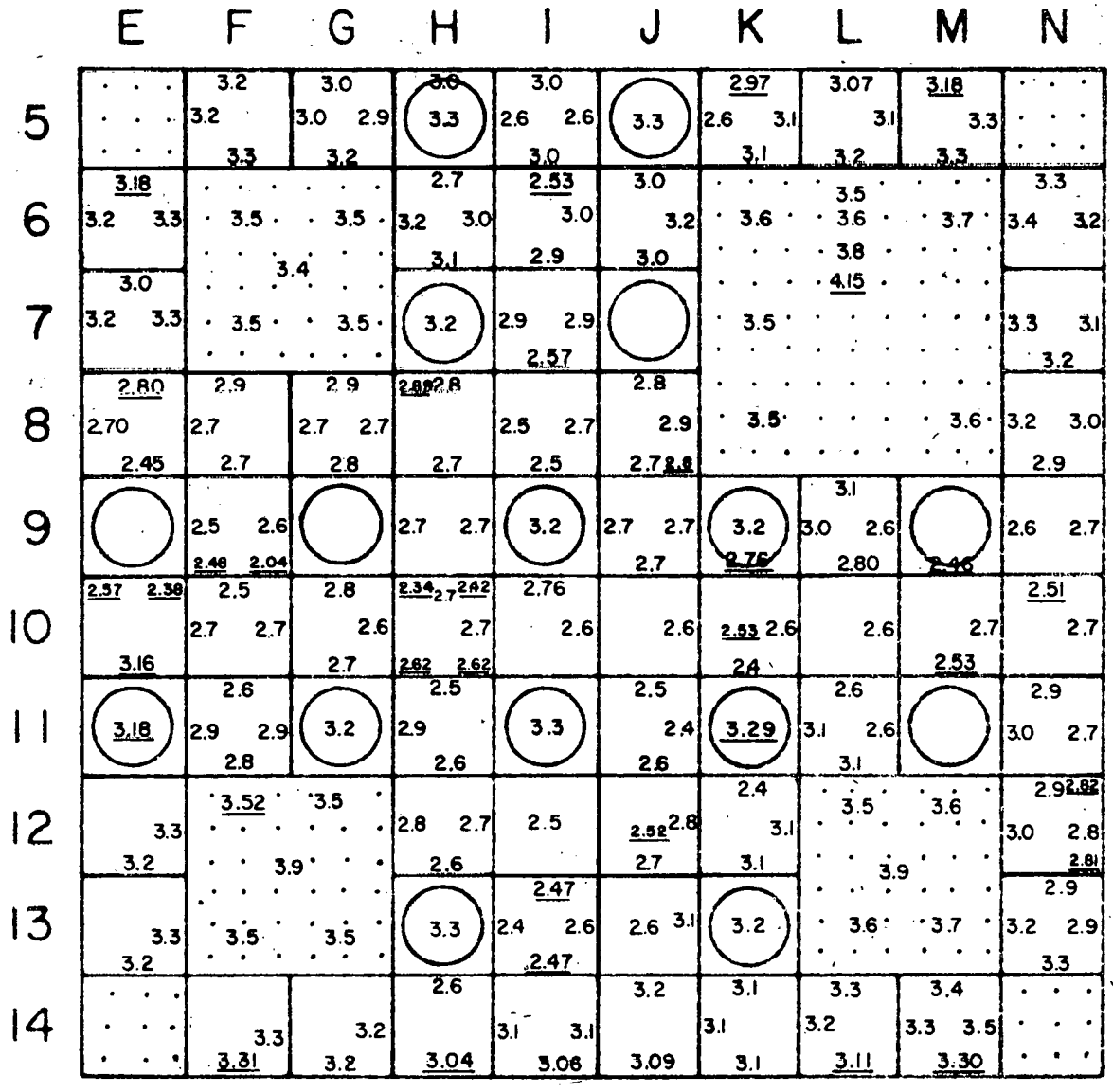

CADMIUM RATIOS

EXPERIMENTAL VALUES ARE UNDERSCORED

FIGURE 2

ETRC CORE

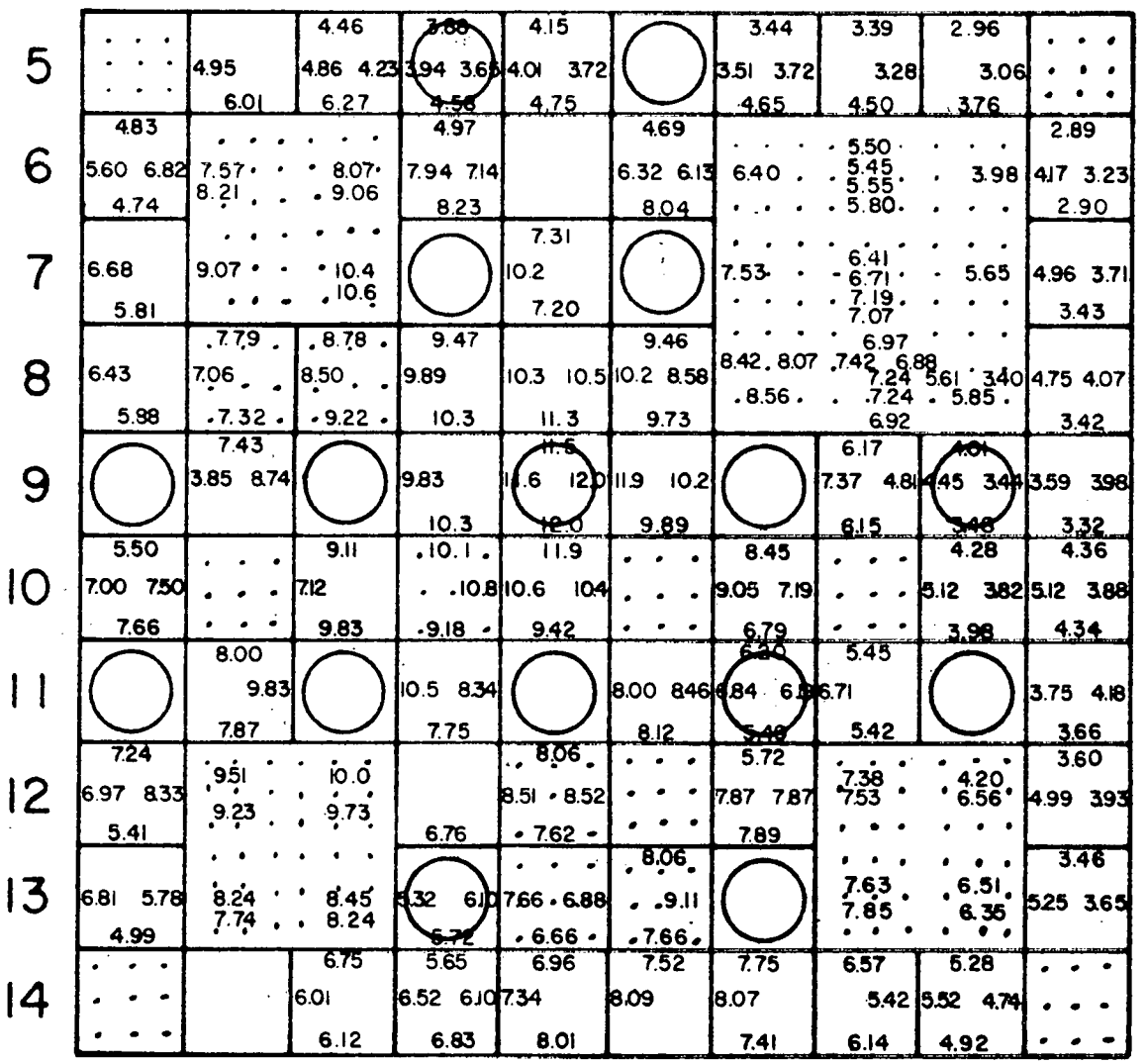

FLUX MAP

THERMAL FLUX AT MIDPLANE (neut./sec./cm^2 10^{-8})

FIGURE 3

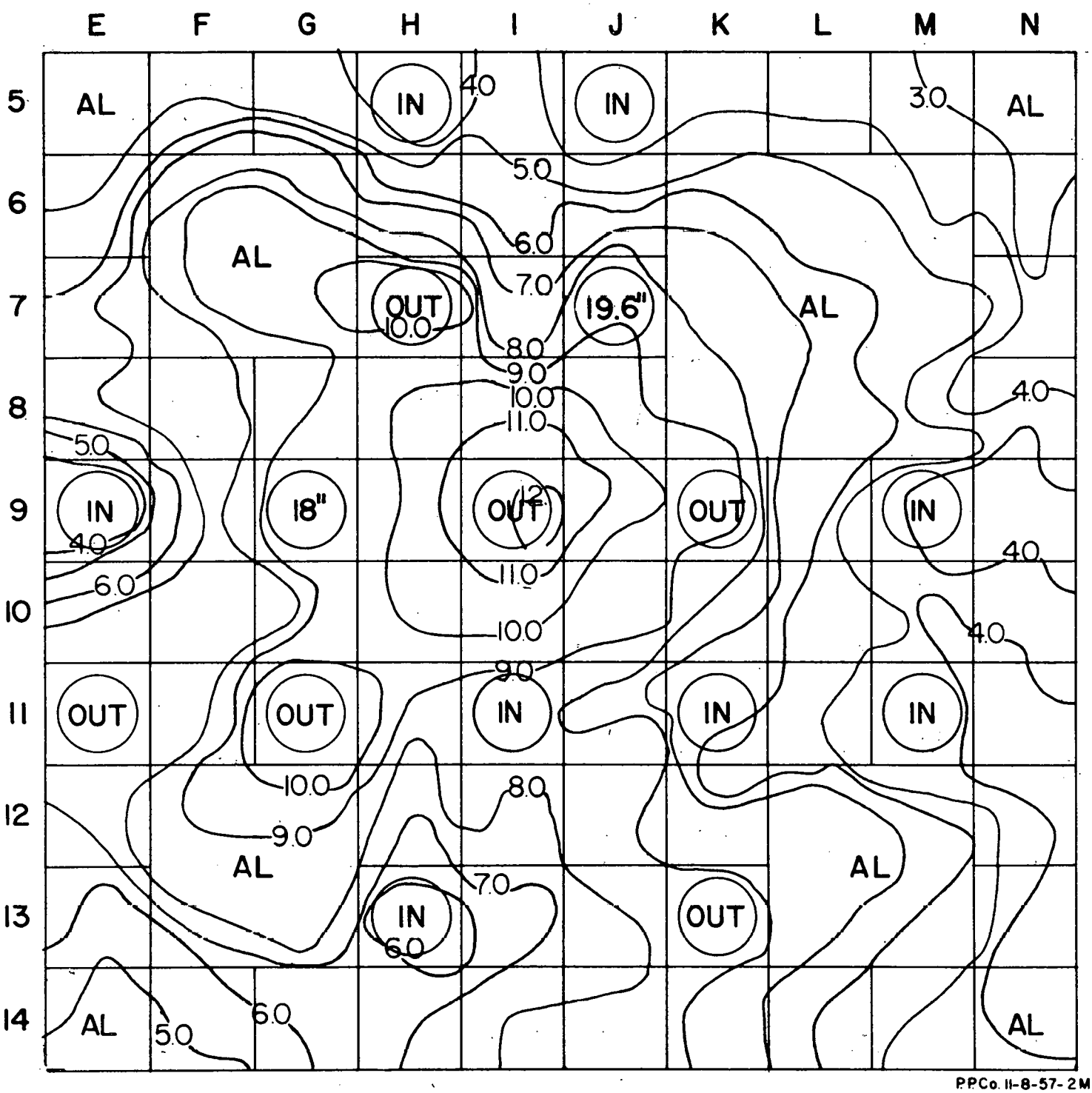

THERMAL FLUX MAP (neut./sec./cm^2 10^{-8})

E.T.R. CRITICAL FACILITY

59 ELEMENT CORE

FIG. 4

FIG. 5

ETRC CORE

VERTICAL FLUX TRAVERSES OF SELECTED ELEMENTS

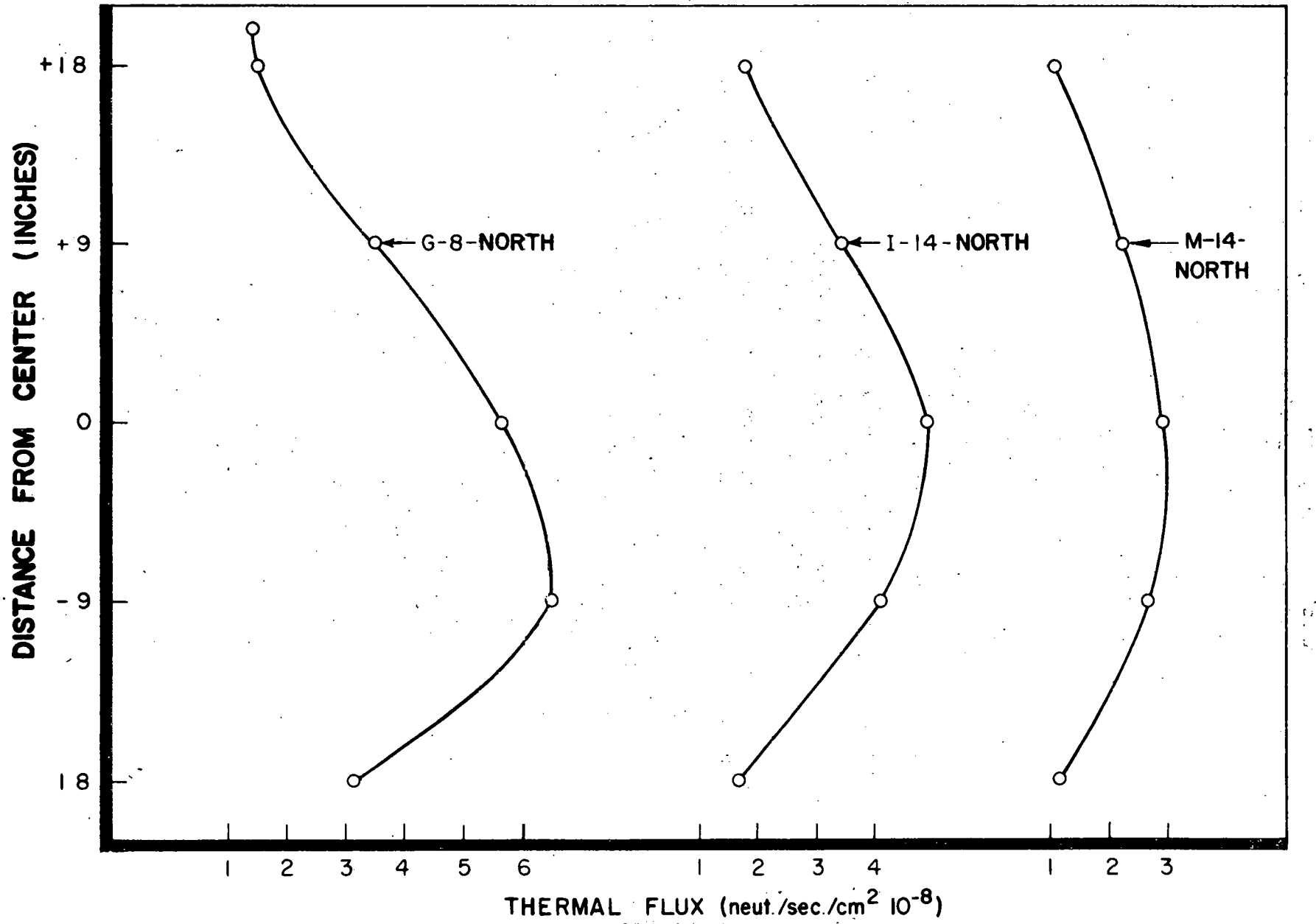

PPCo. 11-27-57-M1

2. Curies of Specific Isotopes (G. A. Cazier, R. W. Goin)

In connection with programing MTR fuel elements for the RaLa process, an equation has been developed which relates the total curies of activity available from an MTR fuel assembly to the number of grams of U-235 consumed.

$$\text{curies} = 1.61 \times 10^{7}\, y_j\, e^{-\lambda_j T_D} \left[\sum_i \frac{\Delta M_i}{t_i} \left(1 - e^{-\lambda_j t_i}\right) e^{-\lambda_j T_i} \right] \qquad \text{II-3}$$

where

λ_j = radioactive constant (hr^{-1}).

y_j = fission yield (fractional).

t_i = length of time for cycle i (hrs).

T_i = time from end of cycle i to end of last cycle (hrs).

T_D = decay time after last shutdown (hrs).

ΔM_i = change in U-235 gram content of assembly in question during cycle i (grams).

This equation has been programed for the IBM-650, and gives the curie content of five species; Ba-140, Sr-89, Sr-90, I-131, and Te-132.

After programing several RaLa elements it was found that a table of curie contents of Ba-140 as a function of all the variables of the above equation would be very useful. Therefore a new IBM-650 program has been developed which calculates the Ba-140 curie content as a function of ΔM_i, t_i, T_i, and T_D. These data has proved to be very helpful in scheduling the RaLa assemblies.

C. Decay Curve Equation (B. L. Hansen)

A "three-component" decay curve may be represented by an equation of the form

$$R = Ae^{-\lambda_a t} + Be^{-\lambda_b t} + Ce^{-\lambda_c t} \qquad \text{II-4}$$

where R is the total activity.

Coefficients of the above equation were derived for curves from five sets of empirical data, using the method of least squares with an incorporated weighting factor.

The empirical data consisted of the total activity (c/m) of a silver sample taken at various time intervals during decay. This equation and the derived coefficients were used to help analyze for mass yields in resonance fission of U-233 (see page 56).

Using decay constants,

$\lambda_a = 3.61 \times 10^{-3}$

$\lambda_b = 2.18 \times 10^{-3}$

$\lambda_c = 6.42 \times 10^{-5}$

Table 2 is a tabulation of the coefficients and associated limits of error (95 percent confidence level) for the five sets of data investigated.

TABLE 2

COEFFICIENTS OF DECAY CURVE EQUATION FOR Ag

Foil	Number	A	B	C
Ag	7-14-57	262.7 ± 57.3	428.2 ± 36.7	66.4 ± 2.5
Ag	7-23-57	46.6 ± 44.3	137.8 ± 31.1	35.2 ± 2.7
Ag	7-30-57	31.3 ± 28.0	87.9 ± 20.1	18.0 ± 1.5
Ag	7-31-57	151.5 ± 48.1	89.6 ± 34.3	36.8 ± 2.9
Ag	8-2-57	44.2 ± 28.3	117.4 ± 20.9	17.7 ± 1.9

D. Machine Computation Facility (M. W. Holm, A. V. Grimaud)

1. General

The volume of work done by the "650" has continued at a high level. In addition to regular (day shift) operations, 88.5 hours of overtime and 139.6 hours of scheduled second shift were used for machine computations.

2. Library Routines

Programs written and/or checked out during this period include the following:

(a) A routine for computing a table of the function A cos BX.

(b) A data reduction routine for the 1024 channel analyzer.

(c) A routine for interpolation using Newton's interpolation formula for fourth, fifth and sixth differences.

(d) L_2, an interpretive system for the 650 obtained from Bell Laboratories.

(e) A routine solving for the quantity $1/\sqrt{E}$.

(f) A routine obtained from ORNL for computing the angular correlation of gamma rays emitted in cascade from excited states of nuclei.

(g) A routine for determining the flux as a function of lethargy.

(h) Paracantor, a two group-two region reactor code obtained from UCRL.

(i) An interpretive subroutine for the solution of systems of first order ordinary differential equations obtained from RCA, David Sarnoff Research Center.

(j) Lil' Abner, a few group one-dimensional code obtained from WAPD.

(k) A tracing routine for normal and interpretive instructions.

3. Machine Utilization

Operating statistics for this quarter are given in Table 3.

TABLE 3

MACHINE OPERATING STATISTICS

Month	Warm-up and Test-deck Time	Scheduled Maintenance	Unscheduled Maintenance	Production Time	Power Failures
July	1.7%	3.5%	6.5%	86.6%	1.7%
August	0.8%	4.2%	5.1%	89.7%	0.2%
September	0.7%	5.8%	9.5%	84.0%	0.0%

4. Production Time

Of the 675.09 hours of production time this quarter, 6.3% were spent in checking out programs, and 93.7% in problem-solving and data reduction. A brief breakdown of the production time follows:

Data Reduction

Cross Sections	16.5%
SPERT	14.3%
ICPP	0.3%
Gamma Ray Spectroscopy	27.9%
RMF	0.8%

Calculations

SPERT I Theoretical Studies	18.7%
MTR "Technical Assistance" Calculations	9.6%
Applied Mathematics Computations	1.4%
Miscellaneous Calculations	0.6%

III. MTR-ETR DEVELOPMENT

A. MTR Development

1. Shim Rod Magnet Design (H. W. Davis)

Upon satisfactory operation of the magnet designed for the ETR Critical Facility Control rods[3], it was decided to incorporate many of the design features of that magnet into an experimental MTR shim rod magnet. The MTR magnets have somewhat different operating conditions from the ETR Critical magnets. A list of some of the features of the experimental MTR shim rod magnet versus those of the existing MTR magnet are shown in Table 4.

TABLE 4

Features of MTR Magnets

Feature	Experimental MTR Magnet	Existing MTR Magnet
Operating Current	120 ma	180+ ma
Inductive Voltage Back Pulse (Without Thyrites)	4.5 kv	12 kv
Case Testing Pressure	125 psi	10 psi
Attrition of Case Due To Each Coil Replacement	0%	25 - 100%
Type of Case Closure Containing Exciting Coil	"O" Ring Seal	Weldment
Total Cost For 5 Coils	$500.00	$1,050.00
Cost of 12 Magnets (1952)	--	$17,479.00
Cost of 10 Magnets (1957)	$10,000.00 (approx.)	

Four of the experimental shim rod magnets have performed satisfactorily since their installation in the MTR on August 27, 1957. These magnets have an average of 58.5 days of operation on the shim rods without failure. The average life of existing magnets in the MTR is 43.9 days. Data taken on October 28, 1957, indicate the experimental magnets will perform satisfactorily for several more cycles. For the three months that these experimental magnets have been used in the MTR, they have had no maintenance which compares to an average of 450 hours for maintenance of the existing magnets during a similar period.

The use of a special cross-linked polyethylene gasket should add even more to the expected life of the experimental MTR magnet. Its resistance to radiation plus many good mechanical properties indicate it to be superior to the material now in use. Also, under investigation is the use of natural rubber "O" rings containing a compound resistant to radiation damage which should endure 10 times the radiation that neoprene or silicone can take and perform properly.

The lower cost of the original magnet, the replaceable coil feature, the negligible maintenance required, and the long life of this magnet should aid considerably in the future operation of the MTR.

2. Calculation of MTR Fuel Charges (H. L. McMurry, G. A. Cazier, R. W. Goin)

Several methods have been presented [4,5,6] for the calculation of MTR fuel charges, but so far no very satisfactory one has been found. From perturbation theory one obtains the following relation for calculating the charge life of a fuel load.

$$T_2 = T_1 \frac{\bar{A}_1}{\bar{A}_2} + \frac{1}{\bar{A}_2} \sum_i \left[M^o_{i,2} - M^o_{i,1} \right] \left[3.19 \left(\overline{\overline{\phi^+_f \phi_s}} \right)_i - 1.64 \left(\overline{\overline{\phi^+_s \phi_s}} \right)_i \right]$$

$$- \frac{1}{\bar{A}_2} \sum_i \left[\Delta M_{i,2} - \Delta M_{i,1} \right] \left[3.19 \left(\overline{\phi^+_f \phi_s} \right)_i - 1.55 \left(\overline{\phi^+_s \phi_s} \right)_i \right] \qquad \text{III-1}$$

where

T_2 = life of charge 2.

T_1 = life of charge 1.

$M^o_{i,2}$ = grams fuel in position i in charge 2 when fuel element was new.

$M^o_{i,1}$ = grams fuel in position i in charge 1 when fuel element was new.

$\Delta M_{i,1}$ = grams burned out of the element in position i prior to charge 2.

$\Delta M_{i,2}$ = grams burned out of the element in position i prior to charge 1.

$$\left(\overline{\overline{\phi^+_f \phi_s}} \right)_i = \sum_J \frac{1}{N} \left(\phi^+_f \phi_s \right)_{i,J} \qquad \text{III-2}$$

$$\left(\overline{\overline{\phi^+_s \phi_s}} \right)_i = \sum_J \frac{1}{N} \left(\phi^+_s \phi_s \right)_{i,J} \qquad \text{III-3}$$

$$(\overline{\phi_f^+\phi_s})_i = \sum_J (\phi_f^+\phi_s)_i \quad U_J \qquad \text{III-4}$$

$$(\overline{\phi_s^+\phi_s})_i = \sum_J (\phi_s^+\phi_s)_i \quad U_J \qquad \text{III-5}$$

N = number of vertical cells in position i.

U_J = fraction of the burnout in the i^{th} lattice location which takes place in cell J of the assembly located there.

$$\bar{A}_2 = \sum_i \left[4.05(\overline{\phi_f^+\phi_s})_i - 1.96(\overline{\phi_s^+\phi_s})_i\right] X_{i,2} \qquad \text{III-6}$$

$$\bar{A}_1 = \sum_i \left[4.05(\overline{\phi_f^+\phi_s})_i - 1.96(\overline{\phi_s^+\phi_s})_i\right] X_{i,1} \qquad \text{III-7}$$

X_i = fraction of the burnout which takes place in the fuel assembly in the i^{th} lattice location.

This represents a refinement over a previous method[6], which was also based on perturbation theory. It has several disadvantages; but the relation can be adapted to cores using fuels other than highly enriched U-235, and is as good as or better than any of the previous methods for calculating charge life.

3. Xenon Override Problem

With the same bases for derivation as the expression for the reactor charge life, the following relation for calculating xenon override was obtained:

$$\begin{aligned} P\left[\sum_m X^*_{J\to m}(\overline{\phi_s^+\phi_s})_m\right]\left[532(e^{-0.0759t}-e^{-0.104t}) + 4.5(1-e^{-0.0147t})\right] \\ + 0.082\, e^{-0.0759t} \sum_m \left[M^{*o}_{m,3}(\overline{\phi_s^+\phi_s})_m - \Delta M^*_{m,3}(\overline{\phi_s^+\phi_s})_m\right] \\ = \bar{A}_1 T_1 + 0.098 \sum_i \left[M^o_{i,1}(\overline{\phi_s^+\phi_s})_i - \Delta M_{i,1}(\overline{\phi_s^+\phi_s})_i\right] \\ - \sum_i \left[\Delta M_{i,3} - \Delta M_{i,1}\right]\left[3.19(\overline{\phi_f^+\phi_s})_i - 1.55(\overline{\phi_s^+\phi_s})_i\right] \\ - 0.017 \sum_m \left[M^{*o}_{m,3}(\overline{\phi_s^+\phi_s})_m - \Delta M^*_{m,3}(\overline{\phi_s^+\phi_s})_m\right] \end{aligned}$$

$$- 0.017 \sum_n \left[M^{**}_{n,3} (\overline{\phi^+_s \phi_s})_n - \Delta M^{**}_{n,3} (\overline{\phi^+_s \phi_s})_n \right] \qquad \text{III-8}$$

$$- 4.5\, P \sum_n X^{**}_{J \to n} (\overline{\phi^+_s \phi_s})_n + \sum_i \left[M^{o}_{i,3} - M^{o}_{i,1} \right] \left[3.19 (\overline{\phi^+_s \phi_s})_i - 1.64 (\overline{\phi^+_s \phi_s})_i \right]$$

where

* fuel assemblies retained from previous charge.

** fuel assemblies brought up from the canal.

i = all positions in the core

m = all positions containing fuel assemblies retained from the previous charge.

n = all positions containing fuel assemblies brought from the canal.

P = power in megawatts

The other notations are the same as for the charge life equation, except it will be noted that here data goes back two charges instead of just one. The reason for this is that charge 2, which has been terminated by the scram, may not have run long enough for an accurate prediction of its charge life to be made.

Using these relations, fairly good results are possible. The charge life can be predicted with a relatively small uncertainty, and the xenon override can be predicted within an uncertainty of ± 2 fuel elements.

The derivation of these relations and the experimental evidence are provided in IDO-16401.(6)

4. Extrapolated Charge Life From Ingrowth of Xe-135 (H. L. McMurry, G. A. Cazier)

Predictions of MTR charge lives are based on the maximum possible life of a completed run. If this run is terminated before its full charge life is realized, it is necessary to estimate how long it could have run. Until now this has been done by extrapolating the observed shim rod position vs. MWD curve to the 30-inch level.

Recently, data on the change in shim rod level with time after reduction in power to N_L (≈ 0.01 of full power) have become available. Following a suggestion of W. B. Lewis, equations based on these data have been developed for estimating the additional time a charge could run following its termination.

An extrapolation of the shim rod vs. MWD curve can be obtained from the relation (7)

$$T_1 = T_1' + 13.4 \frac{\left[\sum_i X_i (\phi_s^+ \phi_s)_i\right] t}{A} \qquad \text{III-9}$$

where

T_1 = total possible MWD from charge 1.

T_1' = actual MWD run of charge 1.

13.4 = constant obtained from solving the transient equations of Xe-135 and Sm-149.

X_i = fraction of burnout in lattice location i.

$(\phi_s^+ \phi_s)i$ = the slow flux weighted by the slow adjoint attributed to lattice location i.

A = number pertaining to the fuel burnout distribution (6).

t = time in minutes at N_L at which shims have reached 30 inches.

Substituting numerical values into equation III-9 we have approximately:

$$T_1 = T_1' + 11.4\ t \qquad \text{III-10}$$

This method of obtaining the total possible MWD's from a given charge has proved to be much superior to other methods.

B. ETR Development

1. Fuel Element Boron Content

a. Evaluation of Boron Measurements (J. A. Merrill)

Experiments were statistically designed to enable evaluation of the relative merits of feasible methods for determination of boron in U-Al alloy. The best method is based upon use of carminic acid. The data were gathered in two stages. Stage 1, covering the first group of 24 experimental runs, constitutes a 2 x 2 x 3 factorial experiment where the factor at three levels (boron) did not have the levels equally spaced. Stage 2 was designed to supply additional information concerning the shape of the relationship between boron concentration and the absorbance reading. Regression analysis of the data yields two empirical equations; one based upon the Stage 2 data alone, this being in a narrow range surrounding the properties of ETR alloy; the second based upon all the data collected.

The stage 2 equation (boron range, 0.025 - 0.040 mg, and aluminum range, 18.4 - 23.4 mg, in ETR type melt samples) is as follows:

$$Y = 1.270 \times 10^{-2} + 1.591 \times 10^{-3} X_2 + 1.411 \times 10^{-1} X_3 + 3.30 \times 10^{-1} X_4 + 4.018 \times 10^{1} X_3 X_4 \qquad \text{III-11}$$

where

Y = absorbance reading

X_2 = aluminum concentration

X_3 = boron concentration

X_4 = carminic acid concentration

The Stage 1 equation (boron range 0.010 - 0.075 mg, and aluminum range, 18.4 - 23.4 mg in the ETR type melt samples) is as follows:

$$Y = 1.583 \times 10^{-2} + 4.928 \times 10^{-3}X_2 + 1.327 \times 10^{1}X_3 + 2.181 \times 10^{-1}X_4 + 4.736 \times 10^{1}X_3X_4. \qquad \text{III-11}$$

Figures 6 and 7 are graphical representations of the estimated relationship between the absorbance readings and boron contents at 21 mg aluminum, and at 0.05 and 0.10 weight percent carminic acid, respectively. The broken lines represent the 95 percent confidence level limit of uncertainty attending a single determination.

b. Boron Contents of B and W "Heat" Samples (F. H. Tingey)

Additional chemical analyses for boron content of Babcock and Wilcox heat samples have been made. The heats involved were so chosen to represent those in which an efficiency of boron retention of 100 percent was assumed. Furthermore as can be seen from the data given in Table 5 the samples were chosen so that a comparison between samples from different ingots of the same heat and samples from different positions in the rolled ingot could be effected. Statistical analysis of the data show that there is as much variation between samples from the same ingot as there is between samples taken from different heats and in fact this variation is in some cases in excess of 100 percent of the average concentration (1.46 mg/g) for the twenty samples.

It is also to be noted that the average concentration, 1.46 mg/g, as found from these samples is still in excess of the specification value of 0.96 mg/g and is not significantly different from the average concentration of 1.49 mg/g found for the 25 sample analyses previously observed for heats in which 75 percent boron efficiency factor was being used. It is apparent therefore that the fabricating technique by which boron is being introduced into the element is not in control and that some alternative scheme must be devised if the boron content per element is to be controlled to within 0.2 gram as defined in the specifications.

Further evidence as to the gross variation in boron content is provided by inspection of ETR fuel element scan data to date which are given in Table 6. The values given are relative to the nominal U-235 content of 254 grams for the arbitrarily chosen standard, H-421; hence a deviation from nominal content for any given element reflects variation between boron

ABSORBANCE DETERMINATION OF BORON IN U-AL ALLOY

FIG. 6

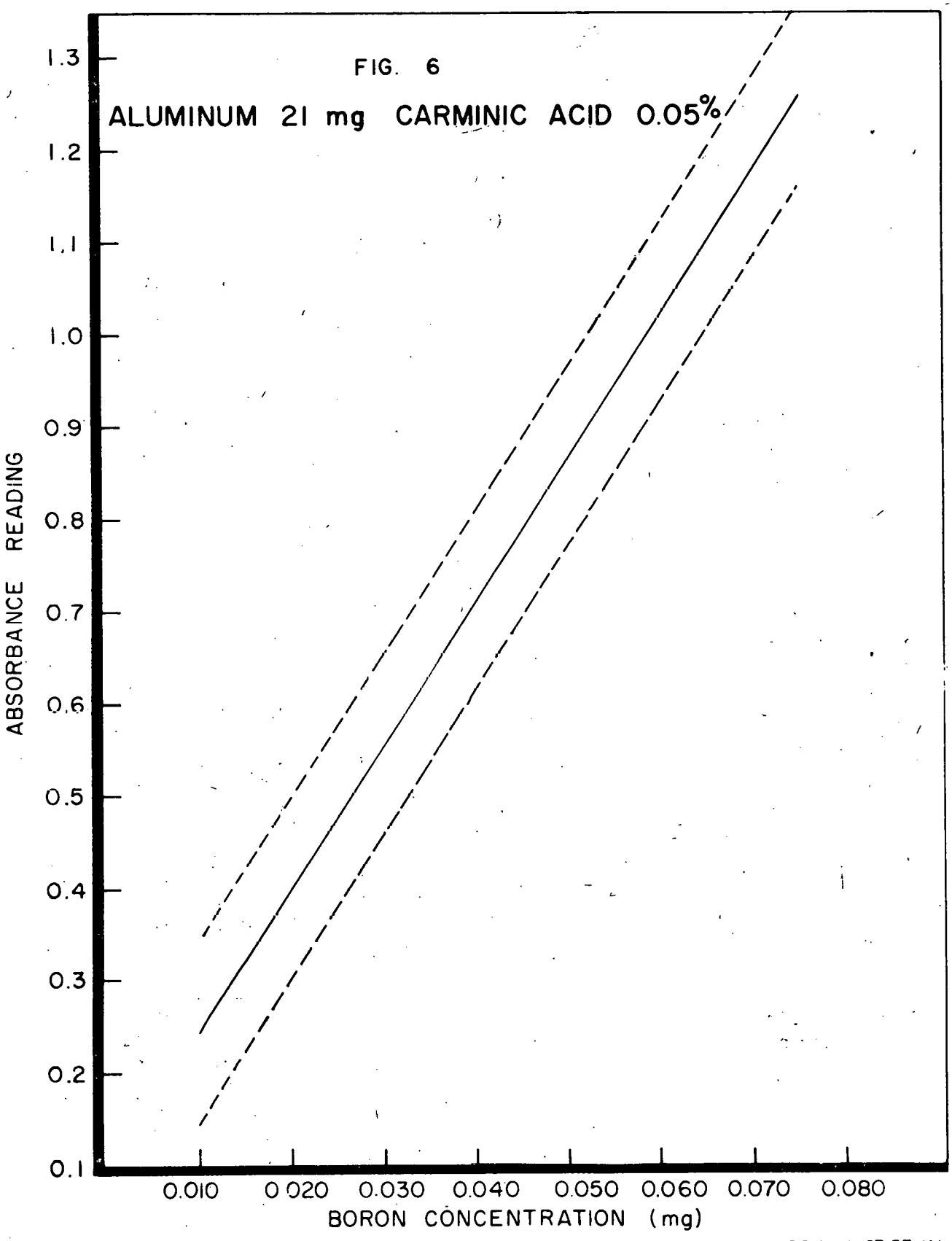

PP Co. 11-27-57-M1

ABSORBANCE DETERMINATION OF BORON IN U-AL ALLOY

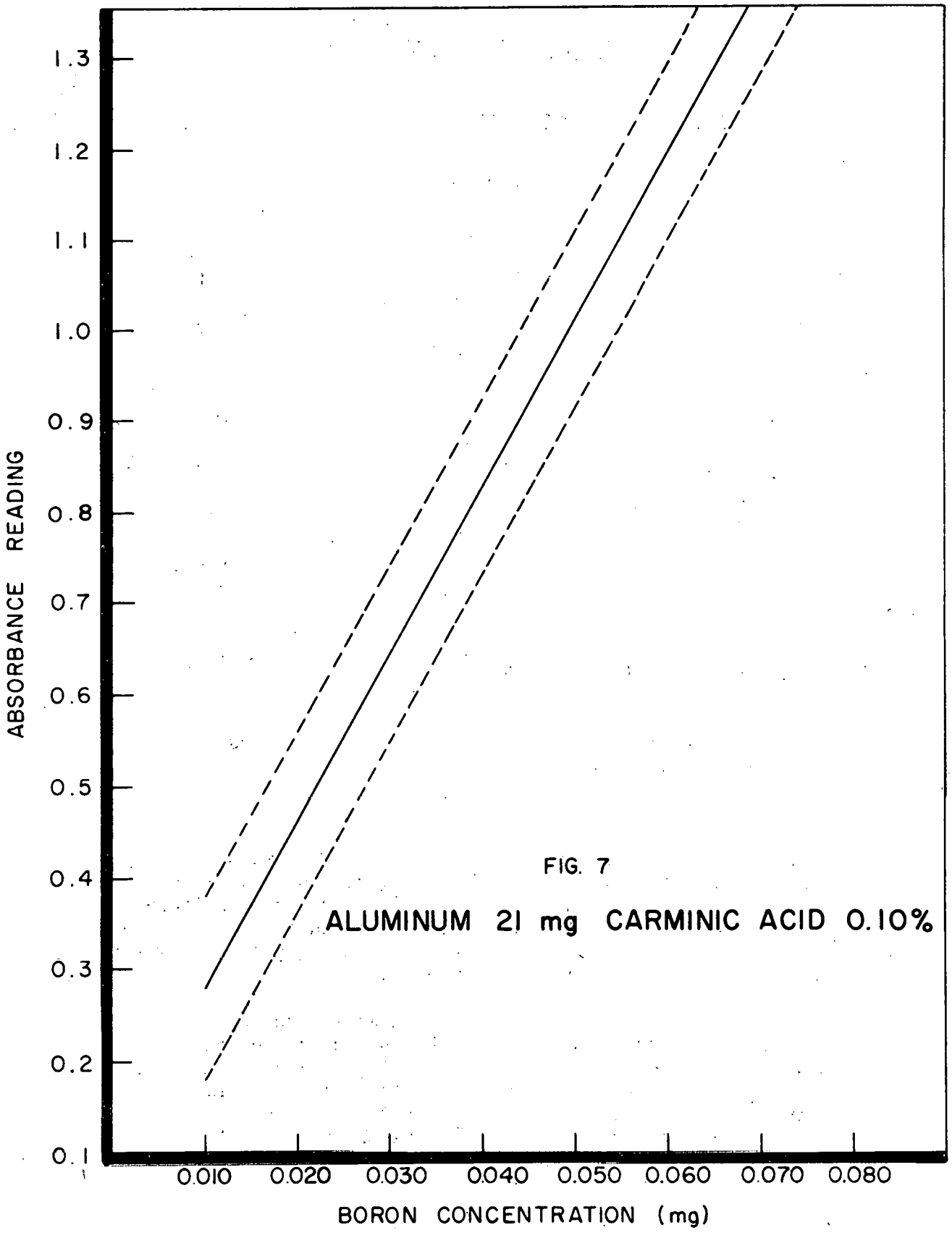

FIG. 7

ALUMINUM 21 mg CARMINIC ACID 0.10%

PPCo. 11-25-57-MI

TABLE 5

BORON ANALYSES ON ETR HEAT SAMPLES

Heat	Ingot	Sample Position	Boron Concentration (mg/g)*
411	1	Top	3.90
	1	Middle	0.20
	2	Top	1.52
	2	Bottom	1.67
414	1	Top	1.29
	1	Bottom	0.80
	2	Top	1.53
	2	Bottom	1.59
425	1	Top	0.90
	1	Middle	0.51
	2	Top	1.46
	2	Bottom	1.77
432	1	Middle	1.62
	1	Bottom	1.08
	2	Top	2.38
	2	Bottom	2.31
436	1	Top	0.31
	1	Middle	2.03
	2	Top	1.09
	2	Bottom	1.14

* Specification value of 1.6 g boron/element corresponds to a concentration of 0.96 mg/g in the core.

content of the standard and the element and/or variations in U-235 content and thus primarily reactivity relative to element H-421. In view of experience with scanning MTR fuels which are boron free, differences of the magnitude observed in ETR fuels are grossly in excess of those which can be reasonably attributed to uranium fabricating process deviations and thus must be attributed to gross boron variation.

Attempts are being made to shed more light on this problem by making chemical determinations of both boron and uranium on samples from those heats involved in the "standard" (H-421) element. In addition, an experiment is being designed to determine the amount of segregation existing in the master alloy used by the fuel element fabricator in the ETR heats. Samples of approximately the same weight as the heat samples will be analyzed for boron content and compared in terms of variation with that observed for the heat samples.

TABLE 6

Element	Scan U-235 Content, Relative to H-421, grams	Shipper's Nominal U-235 Content, grams
H-421	Standard	254.02
H-363	250	253.63
H-370	245	253.03
H-371	254	253.68
H-373	255	253.68
H-378	228	253.42
H-379	252	253.46
H-384	242	253.40
H-386	267	253.19
H-387	251	253.36
H-389	249	254.30
H-392	249	254.44
H-395	253	255.61
H-396	250	253.84
H-397	228	253.84
H-398	253	254.43
H-399	269	254.43
H-400	251	254.13
H-403	249	253.47
H-404	245	253.47
H-405	234	253.47
H-406	267	253.47
H-407	254	256.85
H-408	248	256.00
H-409	236	256.00
H-410	256	256.00
H-411	260	256.00
H-412	243	256.00
H-419	231	255.96
H-420	253	255.68
H-423	263	263.61
H-424	264	255.95
H-425	230	256.16
H-426	245	256.85
H-427	250	256.43

Control Rods	Scan U-235 Content, Relative to H-17, grams	Shipper's Nominal U-235 Content, grams
H-17	Standard	101.81
H-16	98	101.77
H-18	97	101.77
H-19	99	103.40
H-20	99	103.40
H-21	94	103.40
H-22	96	103.40
H-23	104	103.40
H-24	103	101.70
H-25	100	101.70
H-26	101	101.70
H-27	100	101.70
H-28	105	101.60
H-29	105	103.37
H-31	97	103.20
H-33	104	101.92
H-34	98	101.92
H-35	104	101.92

L's	Scan U-235 Content, Relative to L-316, grams	Shipper's Nominal U-235 Content, grams
L-316	Standard	240.91
L-310	273	239.56
L-312	243	237.84
L-317	256	240.91
L-319	247	240.12

2. Fuel Element U-235 Content

a. Delayed Neutron Activation Analysis (C. C. Nielsen)

Experiments were designed and evaluated for determining the effect of the presence of boron and for identifying and estimating the variables in the nucleonic activation technique of determining U-235 content in ETR fuel alloy samples.

To determine the effect of boron, five replicas from each of four boron-spiked uranium samples were prepared for activation. The sample preparation scheme was as follows: from one uranium sample were drawn 5 aliquots, each of which was spiked with a different amount of boron; from each aliquot 4 samples of 250 λ each were pipetted into polyethylene rabbits for activation. The experimental scheme used was that of a randomized-block experiment. For this experiment the different capsules containing the same boron were "blocked" with time in order to determine the effect of boron within the range expected to be found in the ETR fuel samples to be tested. The Analysis of Variance Table showed no significant effect attributable to the presence of boron.

Having determined that boron would have little or no effect on the assaying of fuel samples by this method it was decided to identify and estimate the variables present in this method. For these four samples were prepared containing 0.1, 0.2, 0.3, and 0.4 mg U-235/ml and two aliquots each of 250 λ were pipetted into polyethylene rabbits. These were analyzed using a randomized-block scheme. Within each block each aliquot was duplicated. The analysis of variance listed in Table 7 shows the variables and their estimated mean square variation.

TABLE 7

ANALYSIS OF VARIANCE

Source of Error	Degrees of Freedom	Mean Square Variation
Between uranium concentrations	4	1,202,216,305
Between duplicates	5	482,786
Analytical error	10	145,893

The significance of the sources of error can be tested by dividing the mean square for the variables to be tested by the mean square associated with analytical error. This ratio of the mean square of the variation between duplicates to analytical error is 3.31. A table of the "F" distribution gives a value of 3.33 which shows significance at the 95 percent confidence level. From this table it is possible to ascertain the expected error in determining the U-235 content of a given sample. It was found that this method gives a precision of ± 7 percent stated at the 95 percent confidence level. This figure is estimated using both the analytical error and the sample preparation error.

b. Nucleonic Assay of Reactor Fuel (F. P. Vance, F. H. Tingey)

In connection with liaison on fuel procurement contract C-200 with Babcock and Wilcox Company, most of the fuel elements were scanned on the non-destructive assay facility. Analysis of these data showed that variable fuel core area introduces a large uncertainty in the measurement. The device was accordingly fitted with a drive mechanism that propels the fuel element at a steady speed across the neutron beam. By utilization of instruments available on the Reactor top at the MTR it has been possible to collect a graphical trace of the scan. It is thus possible to compare fuel elements on the basis of total counts, detect apparent anomalies in distribution, and to make precise measurements of mean fuel core length. The total counts collected enables excellent counting statistics; reproducibility is expected to be of the order of $\pm$ 1.5 percent (95 percent confidence level) compared with $\pm$ 2.5 percent previously.

3. Minimum Risk Fuel Element Specification Limits (F. H. Tingey, J. A. Merrill)

A study has been completed in which there were developed methods for establishing rejection limits to be used by the purchaser of a manufactured product in a screening (100 percent) inspection system which minimize the total risk associated with the misclassification of items of product in the presence of measurement variation. It is conceivable that because of measurement error an item is classified as defective when in actuality the item of product possesses a true value for the quality characteristic under surveillance which lies in a region which, from an operational standpoint, has been determined to be acceptable. On the other hand, an item might be classified as nondefective when in actuality the true value for the characteristic is outside the established technical limits. The economic consequences of misclassifying an item of product and the probability that an item would be misclassified formed the basis for defining the risk to be minimized.

The practical problem which initiated this study arose in conjunction with the writing of fuel element specifications for the Materials Testing Reactor and the Engineering Test Reactor.

In addition to developing the methods for establishing the rejection limits, an extensive tabulation of particular solutions was drawn up for the case felt to possess the most desirable properties from the practical standpoint.

4. ETR Storage Rack Calculations (G. D. Marshall, D. R. Metcalf)

It was desired to know under what conditions a criticality hazard might exist in a proposed storage rack to be placed in the ETR canal. This rack consisted of a 6 x 21 array of square cells 3 3/8" on a side. For calculational purposes, the fuel assemblies were assumed to be arranged in rows. These rows were separated by water gaps. Separating each row of fuel assemblies and water gap was a sheet of cadmium. It was necessary to:

(1) determine the critical water gap spacing between the fuel elements in the rack as a function of fuel assembly loading for both boron poisoned elements (1.55 gms per assembly) and elements with no boron.

(2) investigate the variation in water gap spacing for change in metal-water ratios. Spacing values were calculated (with no boron) for metal-water ratios of 0.40 and 0.50 which are on both sides of the 0.46 value used in (1).

a. Methods

The standard two-group diffusion theory equations were applied.

Fuel Region	Water or Moderator Region
$D_{1c}\nabla^2\phi_{1c} - \Sigma_{1c}\phi_{1c} + \nu\Sigma_{2f}\phi_{2c} = 0$	$D_{1m}\nabla^2\phi_{1m} - \Sigma_{1m}\phi_{1m} = 0$
$D_{2c}\nabla^2\phi_{2c} + \Sigma_{1c}\phi_{1c} - \Sigma_{ac}\phi_{2c} = 0$	$D_{2m}\nabla^2\phi_{2m} + \Sigma_{1m}\phi_{1m} - \Sigma_{am}\phi_{2m} = 0$

III-13

This system was assumed infinite in two directions, thus making the flux a function of x only.

Boundary conditions were applied as follows:

(A) Fast and slow fluxes in fuel and moderator are symmetrical for an infinite system about $x = 0$ and $x = b$, where b is the midpoint of water slab and $x = 0$ is at the center of fuel slab.

(B) Continuity of fast current and flux at $x = a$, where a is the boundary between fuel and water region.

(C) Slow flux in fuel is set equal to zero at $x = n$, i.e., $\phi_{2c}(n) = 0$, where $n = a + 0.71\,\lambda_{tr}$.

By applying boundary condition A, the following flux equations are determined:

$$\phi_{1c} = A\cos\mu x + B\cosh\nu x$$

$$\phi_{2c} = AS_1\cos\mu x + BS_2\cosh\nu x$$

$$\phi_{1m} = C\cosh k_{1m}(x-b)$$

$$\phi_{2m} = R\cosh k_{2m}(x-b) + S_3\phi_{1m}$$

III-14

$$k_{1m}^2 = \frac{\Sigma_{1m}}{D_{1m}} = \frac{1}{\tau_m}\ ;\ k_{2m}^2 = \frac{\Sigma_{am}}{D_{2m}} = \frac{1}{L_m^2}$$

Boundary conditions B and C were applied, from which a determinant for criticality was derived:

$$\begin{vmatrix} \cosh \nu a - \frac{S_2}{S_1}\frac{\cos \mu a}{\cos \mu n}\cosh \nu n & -\cosh k_{1m}(b-a) \\ D_{1c}\mu \frac{S_2}{S_1}\frac{\sin \mu a}{\cos \mu n}\cosh \nu n + D_{1c}\,\nu \sinh \nu a & D_{1m}k_{1m}\sinh k_{1m}(b-a) \end{vmatrix} = 0 \qquad \text{III-15}$$

The volume of a cell was taken to be 6,720 cm^3. The microscopic cross sections used to compute the constants of the determinant were obtained from BNL-325.(8) The neutron age for the determination considered in (1) above was obtained from the ETR Final Physics Report,(9) while the neutron ages for the investigation in (2) above were taken from IDO 16133.(10) The method was further refined in (2) by considering variation of D_{2c} with U-235 loading. In both (1) and (2), a was 4.32 cm, and b was initially 9.40 cm.

b. Results

The results are shown in Figures 8 and 9 with the safety factor of no leakage in y and z directions included in the model. Water gap spacings above the criticality curves will thus be safe (not critical according to the two-group model. A metal-water ratio change of 10% resulted in 5% change in water gap spacing.

C. Fuel Element Development (W. C. Francis)

1. Introduction

The development of fuel assemblies and shim rods for reactors involved hydraulic tests on ETR tank components, design studies on new fuel element and shim rod geometries, and metallurgical testing of sample fuel plates. The out-of-pile, preneutron hydraulic tests provide knowledge of the operating (strength) capabilities of these components. The sample test plate program is aimed at producing an improved fuel element not only applicable to the MTR and ETR but for the AEC reactor program in general. The shim rod modifications are for improvement of MTR control rods.

2. Hydraulic Tests (J. R. McGeachin, A. W. Brown, D. E. Williams)

a. ETR Core Pieces

Pre-neutron, out-of-pile hydraulic testing of the ETR-simulated-beryllium-reflector piece has been completed. Three separate tests (flow versus Δp) have been run on the beryllium reflector piece, consisting of (1) all flow through the four small holes and through the large hole at the center, (2) the flow with the large center hole plugged and (3) flow with a beryllium X-basket located in the center hole. Two separate tests (flow versus Δp) have been run on the aluminum reflector piece. These consisted of one run with and one run without the X-basket located in the center hole. One test (flow versus Δp) has been run on the core filler piece. The core filler piece and the aluminum reflector

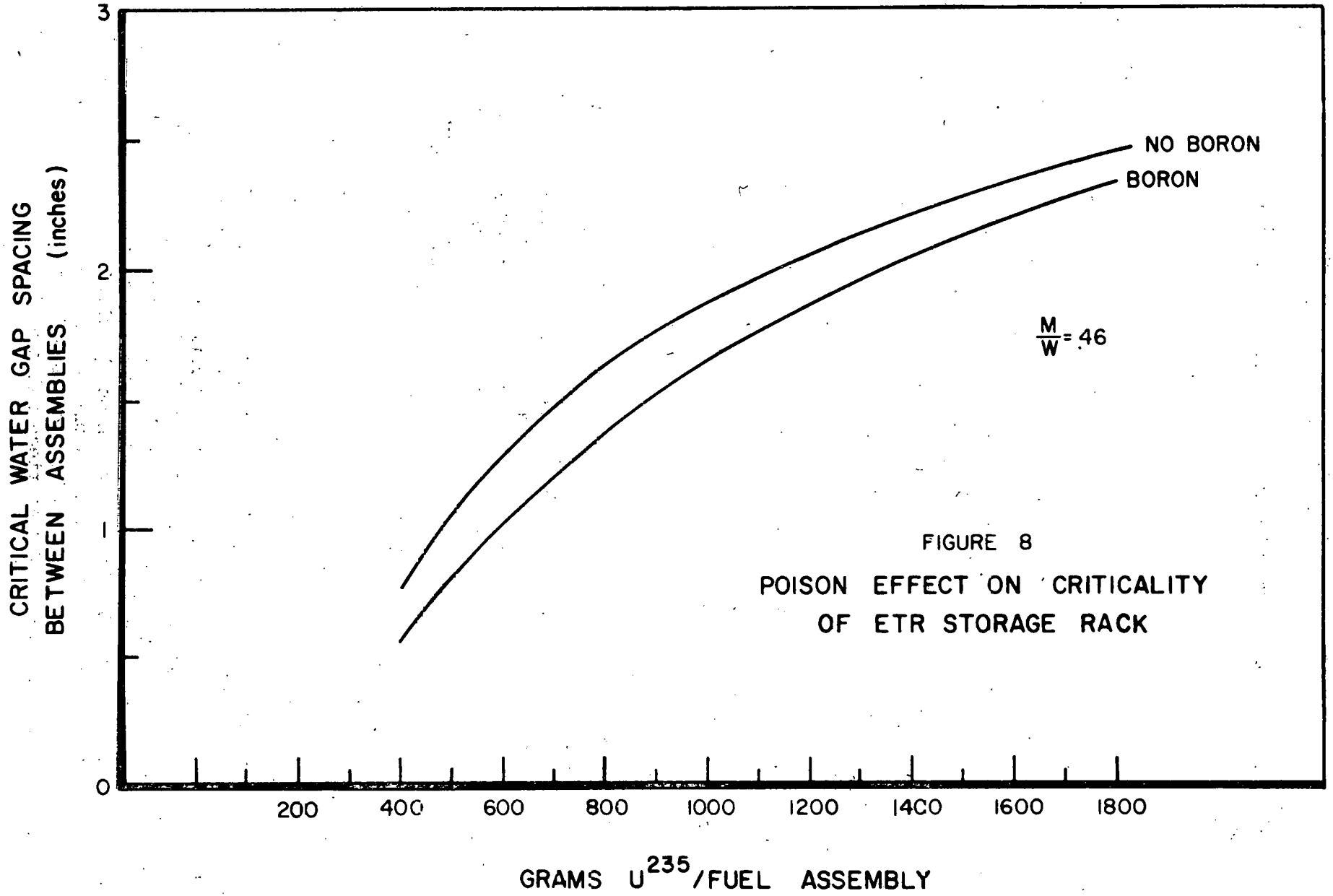

FIGURE 8

POISON EFFECT ON CRITICALITY OF ETR STORAGE RACK

PP Co. 12-18-57-M1

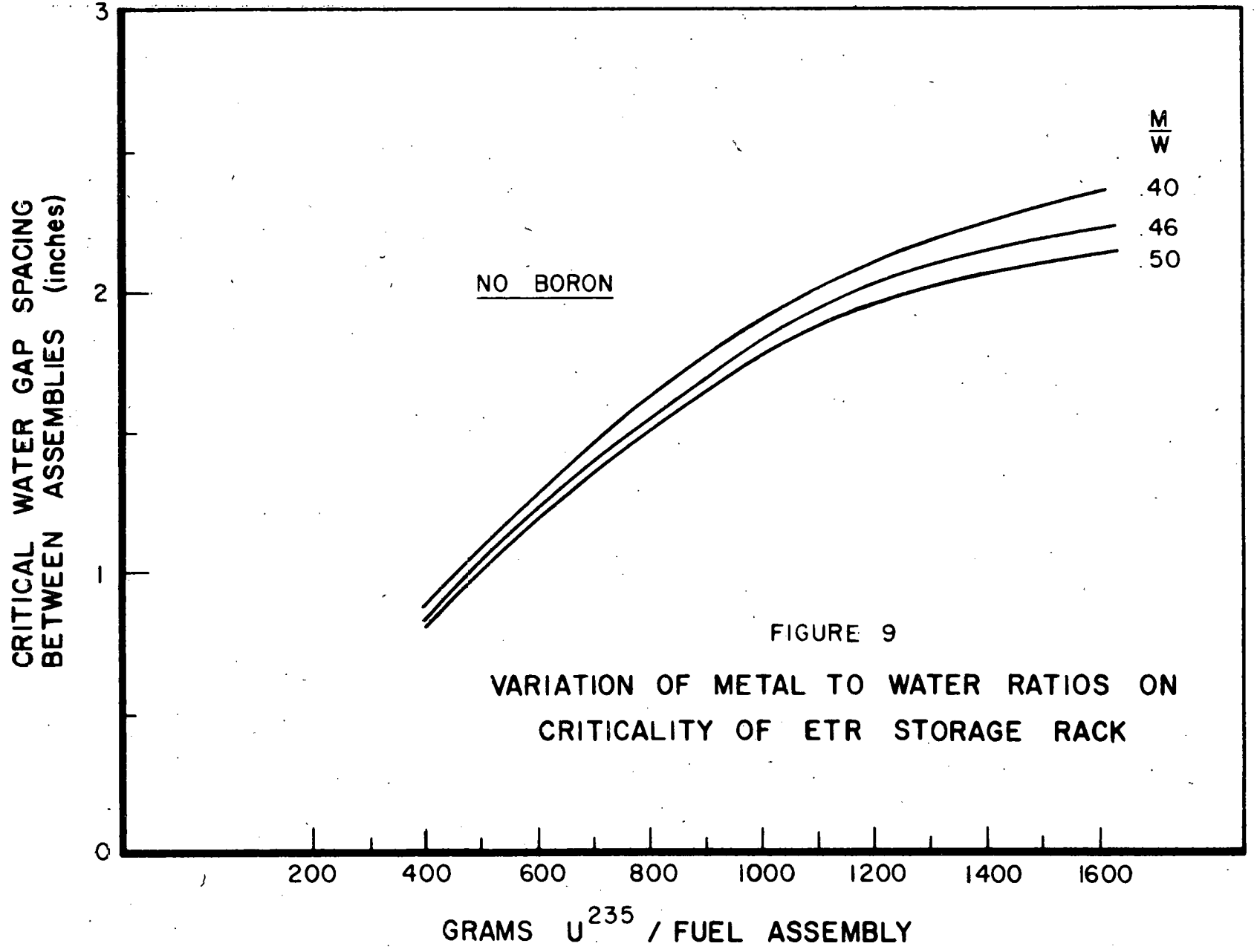

FIGURE 9

VARIATION OF METAL TO WATER RATIOS ON CRITICALITY OF ETR STORAGE RACK

PP Co. 12-18-57-M1

piece were both tested at two different temperatures while the beryllium reflector assembly was run only at one temperature. The flow through the 0.167" hole with the basket in place was 48 gpm and the flow through the 1/4" coolant holes was 34.5 gpm (for a core pressure drop of 55 psi at 70°F and an equivalent fuel velocity of 35 ft/sec). The flow through the core filler piece and aluminum reflector piece was 127 and 26.7 gpm respectively. These results have been forwarded to ETR operations.

b. ETR Single Element Test

Six ETR fuel elements have been tested in the single element hydraulic loop. The elements tested consisted of two with slotted side plate modification, two instrumented for pressure drop along five channels in the fuel section, one wire-braced element, and one production type element. Most tests were run at two different temperatures. The change of measured pressure drop due to the change of temperature of the coolant agreed with the calculated value. Figure 10 gives the results of the slotted element tests and instrumented element test. All the runs have been corrected to a water temperature of 118° F.

c. Fuel Element Tests in Multi-Element Hydraulic Test Loop

Previous hydraulic tests[11] indicated fuel element failure in the range of 33 - 35 ft/sec. Four tests have since been made with modified ETR fuel elements to determine which of several proposed methods of modification would produce a stronger element. These tests were made in the multi-element hydraulic test loop. The first test utilized four elements which had 0.092 inch aluminum wires fastened between each of the fuel plates and running the entire length of the plates. The capacity of the loop limited the maximum flow which could be obtained to 41 ft/sec through the elements. This flow had been maintained for several hours when pieces of wire were noticed on the top of the fuel elements. The loop was then shut down and the elements examined. Some waviness was observed in the plates of all elements but by far the greatest damage occurred to one dummy element. Three of the wires in the center channels of this element had broken off and the plates bulged, restricting flow in these channels. Many wires in the outside channels stretched or cut into the comb on which they were hung until they were quite loose over the plate. Definite scar marks along the outside plates indicated the wires underwent considerable vibration and that this occurred generally towards one edge of the plate. The broken wire ends indicated fatigue failure.

The second test utilized elements with square spacers brazed between each of the fuel plates in five elements. These spacers extended down 12 1/2 inches from the top of the fuel plate and 6 1/2 inches up from the bottom, thus leaving 18 inches of unsupported plate (designed so for heat transfer purposes). These elements failed at a velocity of about 35 ft/sec. Examination of the elements revealed extensive damage to the unsupported portion of the fuel plates and little or no damage to the supported sections. However, one of the bottom spacers in one of the elements had been firmly brazed only at the bottom. The flow forced this spacer over to the side plate thus blocking off one-half of the channel. Figure 11 is a photograph showing the results of this failure.

FIG. 10

HYDRAULIC TESTS
ETR SLOTTED ELEMENTS

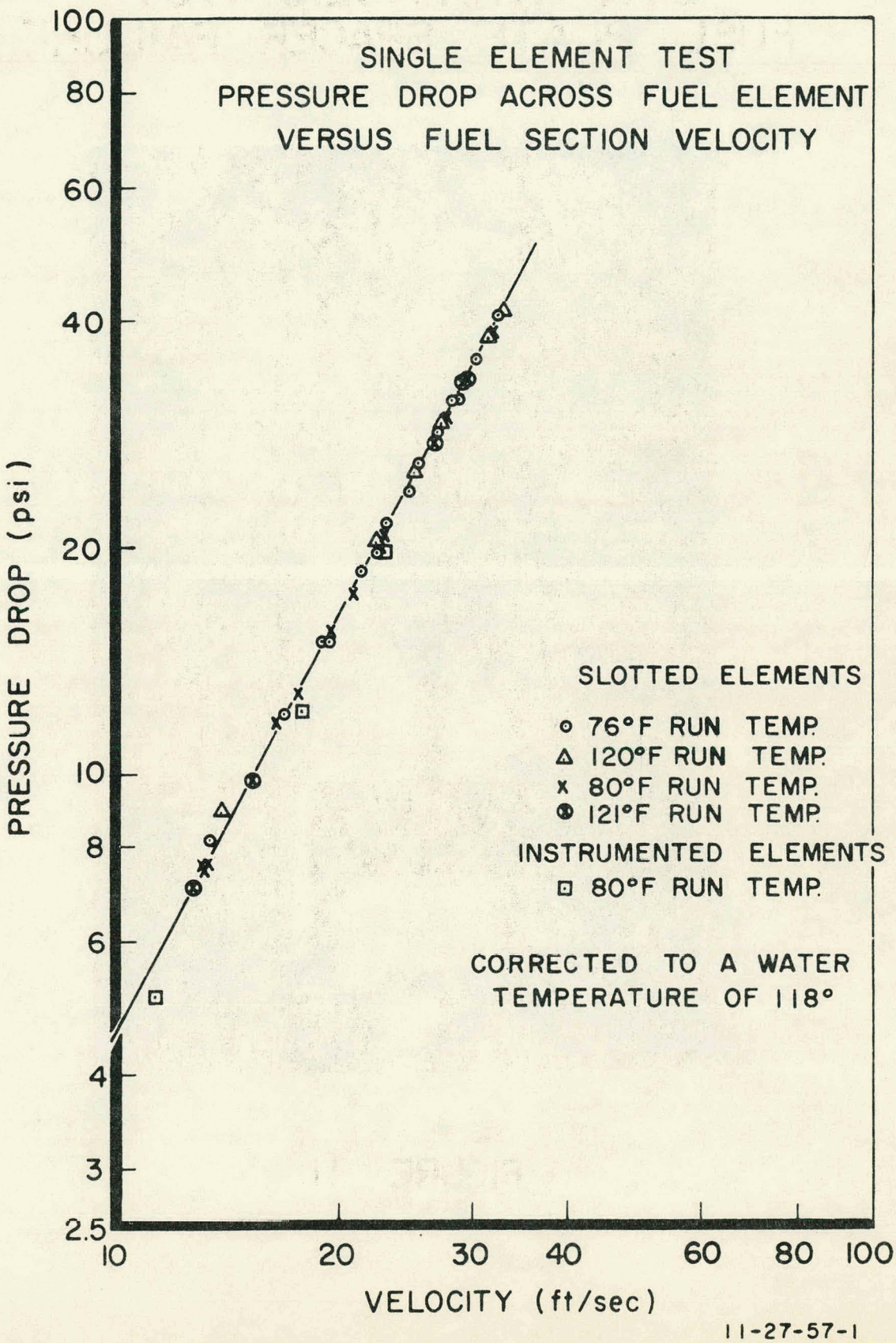

11-27-57-1

ETR HYDRAULIC TEST
FUEL PLATE SPACER FAILURE

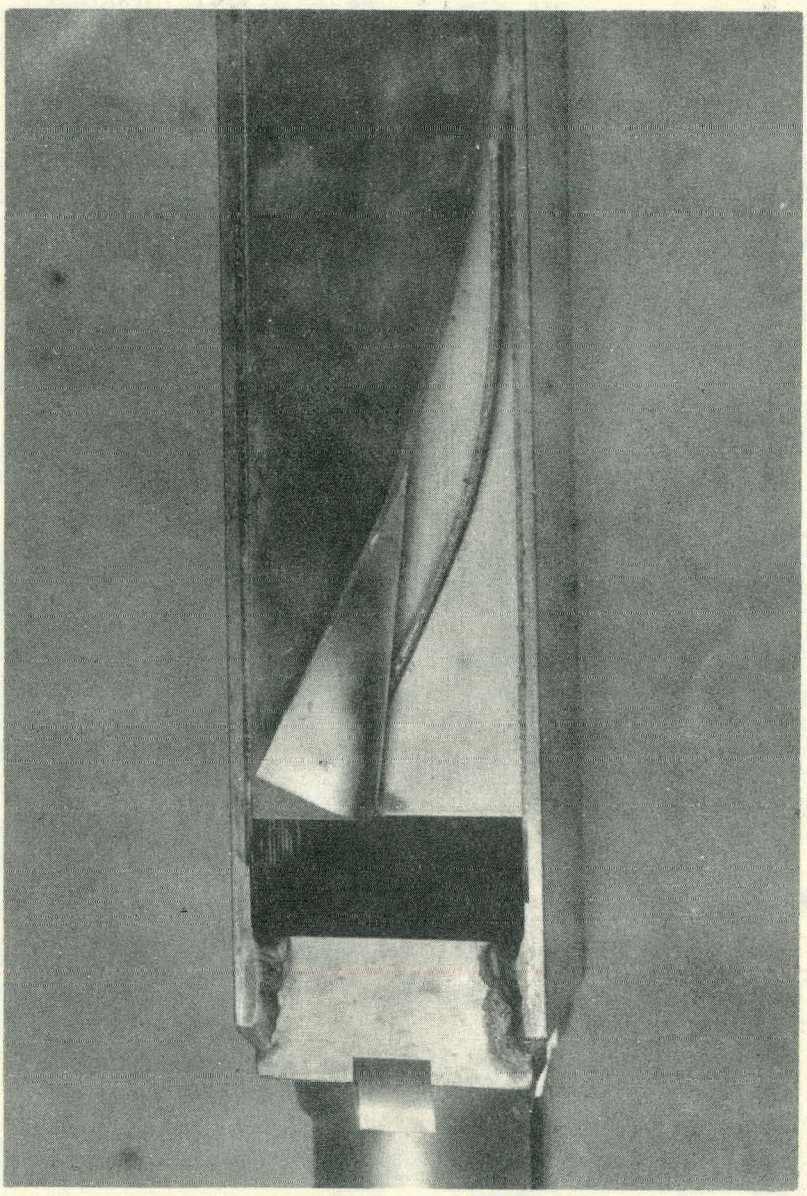

FIGURE 11

The third test utilized three elements with slits cut through the side plates. These slits provided a cross-flow across any given fuel plate if a lateral pressure differential did exist, thus reducing the lateral differential pressure to a minimum. Again the capacity of the loop limited the maximum flow to 42.7 ft/sec. Inspection of the elements at the end of the test revealed that no damage had occurred.

The fourth test utilized three elements furnished by GE-APED. The fuel plates of the elements were cold rolled and swaged into the side plates of the fuel assemblies. This method of fabrication omits the brazing step and permits the use of cold work hardened plates. The maximum flow obtained during this test was 43.9 ft/sec (higher than the previous test due to increased system pressure and reduction of back-pressure in the bottom end box). No damage was sustained by any of the elements during the test.

The method used to compute the velocity took into account the flow through the core but external to the elements themselves. This was done by obtaining one equivalent channel external to the fuel element channels and then assuming that the friction drop in this equivalent channel is the same as the friction drop in a nominal (0.110 inch) channel within a fuel assembly. The equivalent diameter of this external channel was obtained by summing the perimeters of all the core pieces, the external perimeter of the fuel elements and the reflector perimeter, then using as the area term the available flow area external to the fuel elements.

Figure 12 is a plot of the velocity versus core Δp obtained during five element runs and three element runs. The Δp values have been corrected to a water temperature of 118°F in all cases. As a check on the above method of velocity computation, the five element and three element runs were plotted on a graph of Δp versus core GPM as shown in Figure 13. The difference between these two curves is the flow through just two fuel elements. This can then be related directly to velocity by the flow area within the two fuel elements. The difference between the two curves shown in Figure 13 yields the same velocity curve given in Figure 12.

3. Variable Channel Tests (A. W. Brown)

A variable channel test rig was initially fabricated to simulate various rectangular channels anticipated in the ETR tank. Test runs were made yielding Δp versus flow data. The tests also were used to determine the friction factor versus Reynolds number for water in rectangular channels.

All of the tests utilized a channel length of 37 inches. Four different channel cross sections were tested with aspect ratios (ratio of channel width to breadth) varying from 10.6 to 53.2.

The friction drop was measured by a set of static pressure taps located 5 inches down from the channel entrance and 3 inches up from the exit. The friction factors were determined from the Fanning friction factor equation:

$$F = \frac{2fL\,V^2}{g\,D_e}$$

FIG. 12

ETR HYDRAULIC TESTS

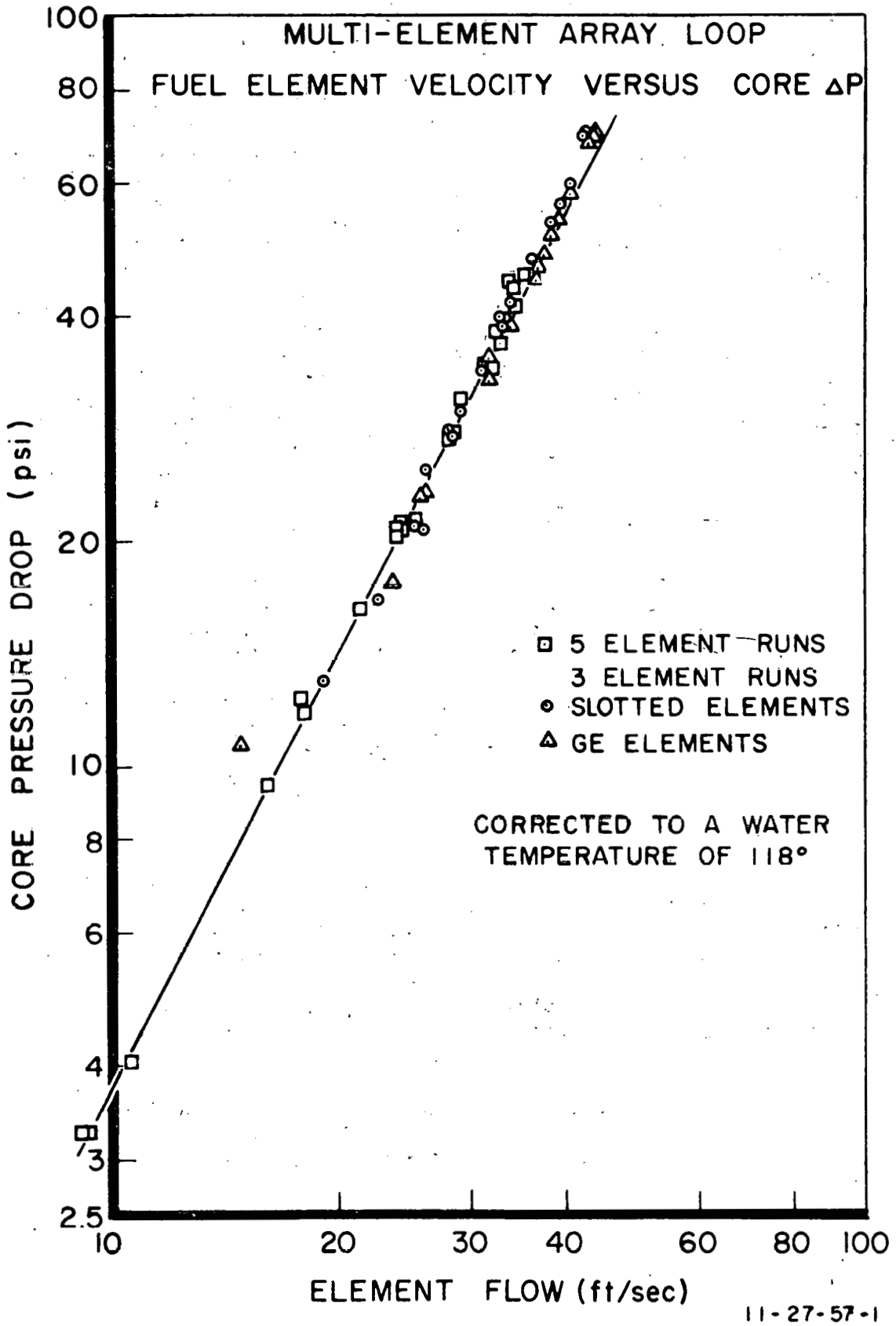

FIG. 13

ETR HYDRAULIC TESTS

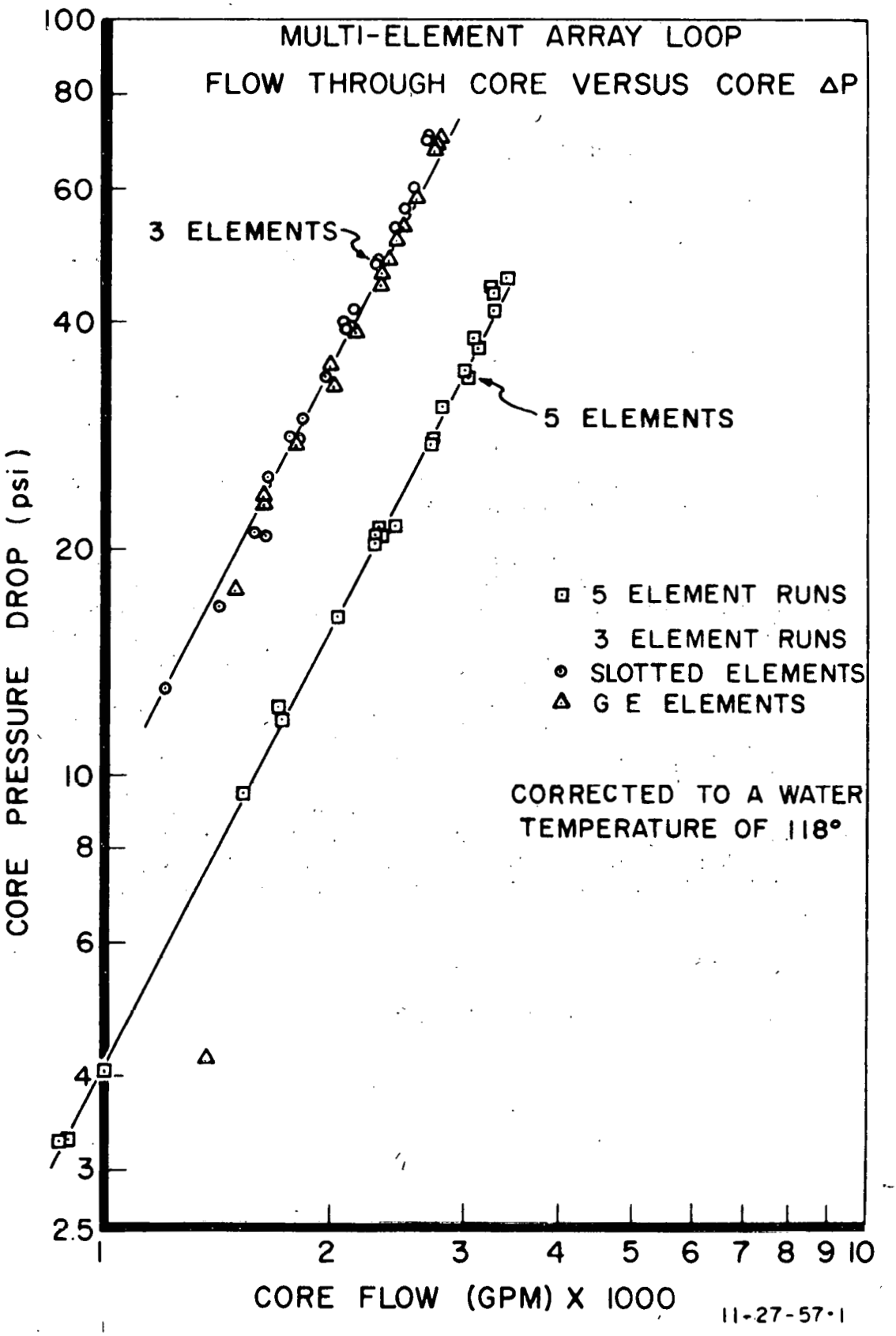

where

f = Fanning friction factor (dimensionless)

F = friction loss (ft of water)

L = channel length (ft)

V = water velocity (ft/sec)

$g = 32.2 \frac{\text{lbs. mass - ft.}}{\text{lbs. force - sec}^2}$

D_e = equivalent diameter (ft)

Figure 14 gives the results obtained for the four channel cisco tested with water temperature of 100° F to 150° F.

The data is best represented by the equation:

$$f = 0.00240 + 0.358 \left(\frac{1}{N_{R_e}}\right)^{0.437}$$

N_{R_e} = Reynolds number.

For comparison purposes, Figure 14 also gives the curves for smooth tubes and commercial pipes.(12)

The design was completed and material ordered for a test fixture very similar to the existing single channel test fixture but made of a special clear plastic possessing surfaces comparable in smoothness, luster, and chemical resistance to polished plate glass. Its resistance to abrasion, wear, and weathering is intermediate between the better grades of thermoplastics and plate glass. Flow patterns are hoped to be observed through use of dyes or particle additives and photographs.

4. Sample Fuel Plates (J. A. Alexander, E. H. Porter, W. C. Francis)

Pre-irradiation metallographic examination has been completed on representative sample plates of the different fuel compositions. The cores all contain UO_2 in various enrichments and weight percentages; several of the cores also contain gadolinium and boron poisons. All plates are clad with aluminum.

The tests completed to date include:

a. Dimensional stability - pre-irradiation measurements of overall dimensions.

b. Uniformity of fuel distribution - examination of radiographs supplied by vendor and metallographic examination of plate cross sections.

FIG. 14

FANNING FRICTION FACTOR VERSUS REYNOLDS NUMBER

RECTANGULAR CHANNELS WITH ASPECT RATIOS FROM 10.6 TO 53.2

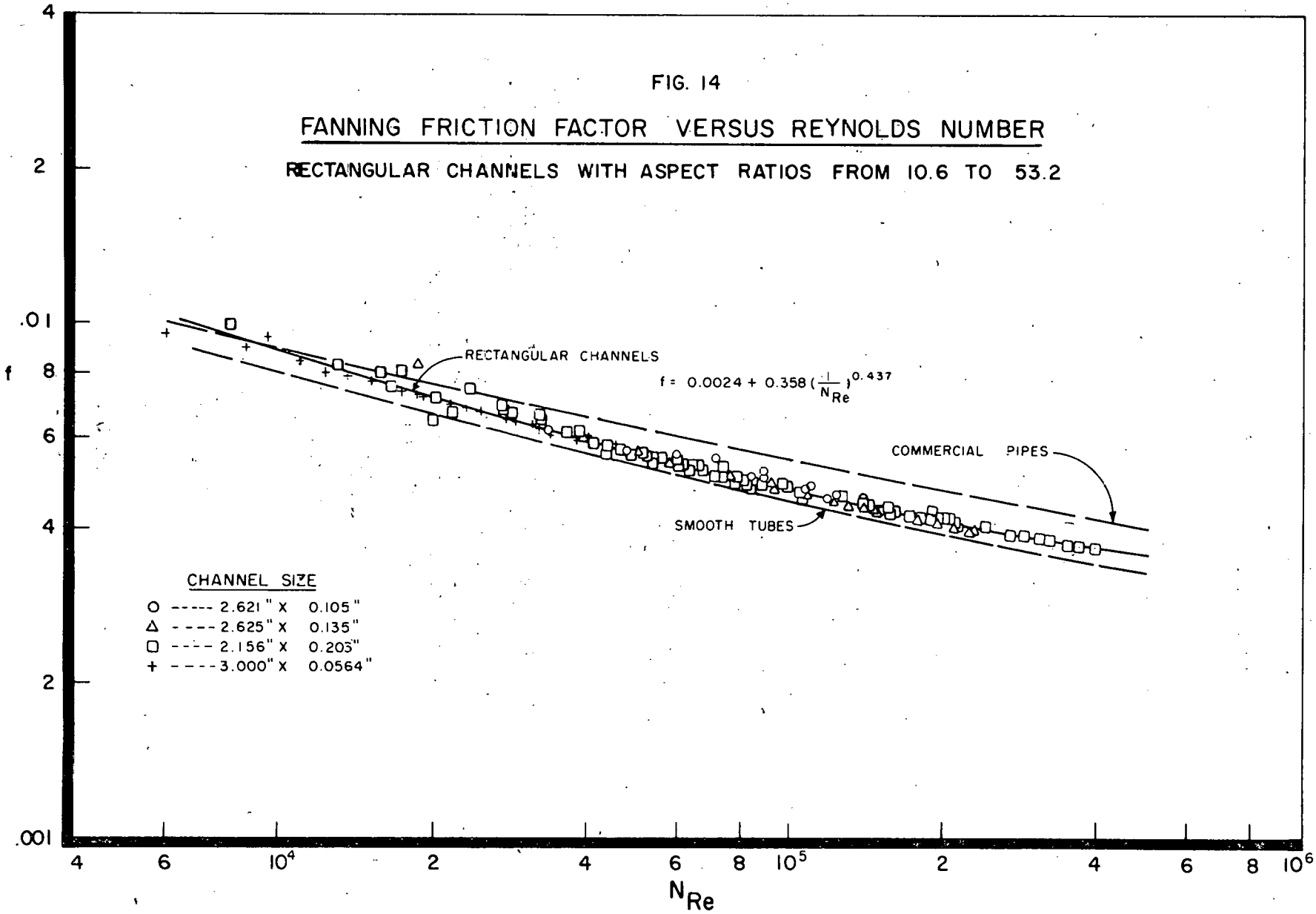

c. Hardness measurements of core and cladding - diamond pyramid hardness measurements have been taken on the core components and the cladding.

d. Photographic record of core and cladding - photomicrographs of core components and cladding have been completed.

Three additional pre-irradiation tests are planned - a furnace blister, an ultrasonic, and a corrosion test. The blister test will furnish information on the quality of the bond between the core and cladding and will eliminate those fuel plates most susceptible to blistering in the reactor. The ultrasonic test is a non-destructive method for determining fuel plate cladding thickness, core thickness, fuel distribution, and quality of the core-to-cladding bond. The latter equipment has been received and is being checked out and adjusted.

Conceptual design is completed for a test corrosion loop providing water velocities of 40 feet per second at 500°F and 1000 psi. The loop will accomodate standard ASTM round tensile test specimens as well as the flat plate test specimens. The loop is closed, with a portion of the water by-passing through ion exchangers to maintain approximately 1.0×10^6 ohm-cm demineralization.

Hot spot - hot channel calculations[13] were made for the reactor insertion of the sample fuel plates for a typical representative L piece loading. Calculations were based upon a known average water velocity of 20.5 feet per second for a given pressure drop across the L piece holder of 40 psi. These data were obtained from flow tests. A typical L piece holder loading was selected and the q/A, Δt bulk, and Δt film were checked for this loading. The loading for each subsequent irradiation will be similarly checked. The experiment now awaits insertion approval, and scheduling.

Arrangements have been made with the vendor of these sample fuel plates to extend the contract to supply the remaining 250 plates originally planned. Because of the difficulties encountered in obtaining test specimens, the feasibility of making them locally has been investigated. A preliminary conceptual layout was made for a facility for fabricating experimental sample fuel plates, rods, and tubes. Cost estimates and technical data were obtained on major pieces of equipment for the facility.

5. MTR Shim Rod Modifications (E. H. Porter, J. A. Alexander)

Heat transfer calculations made on a modified MTR shim rod embodying removable fuel and poison sections have been reported previously.[14] These calculations indicate acceptable flow rates, heat fluxes, and heat transfer rates for a 16 curved plate fuel section. Accordingly formal designs are being completed utilizing much of the previous work but including the following additional features:

a. Removable (and invertable) 16 curved plate fuel section.

b. Removable (and invertable) metal sprayed cadmium poison section.

(Both of the above units are to be removable through the existing upper grid

bearing configuration. Preliminary interference layouts were made to confirm the feasibility of this).

Upon completion of design and drawings a complete prototype shim rod is planned for flow testing. For this purpose, fuel and poison sections will be simulated.

Design and working drawings were completed for the metal sprayed poison section which would replace the present poison section in the shim rod. Metallographic examination has been completed on these sprayed poison sections and a formal report of the results is in preparation. Two designs were examined, viz., (1) an extruded aluminum-sprayed cadmium-sprayed stainless steel section and (2) an extruded aluminum-sprayed cadmium-sprayed aluminum section. Both sections were autoclaved in water at 400° F for 72 hours. The aluminum-cadmium-stainless steel section resisted corrosion well but the aluminum-cadmium bond was very poor and separated easily. The sprayed aluminum layer of the aluminum-cadmium-aluminum section showed serious corrosion and poor bonding. Complete deterioration of this layer could be expected with additional time in the autoclave.

6. Fuel Element Geometries (M. L. Griebenow, F. A. Meichle)

A study of some of the most frequently considered fuel element designs has been conducted, with the emphasis placed on the possible improvement of the ETR. The effects of varying the parameters and bracing or slotting the present flat plate element were analyzed and the possibility considered of a design constructed of bundles, concentric tube nest, or a hexagonal arrangement.

Slotting of the side plates presently in use in the ETR appears to be a simple means for lateral pressure relief. For higher powers, other geometries appear more efficient and several of these are scheduled for further hydraulic tests. The hexagonal arrangement seems to offer considerable promise if some obvious fabrication difficulties can be overcome.

A heat flow simulator was constructed to help determine whether a strengthening brace, tying together the centers of the fuel plates on ETR elements, will cause hot spots at the junction of the brace with the plate. An electrical analog was used to determine the heat flow from the fuel plate through the brace into the water. This two-dimensional analog simulates heat flow through a cross-section of the brace perpendicular to the plates at the mid-plane of the fuel elements. The instrument consists of a resistor matrix in which the resistors simulate the heat flow resistance, current flow simulates the heat flow, and voltage differential simulates the temperature differential.

D. Metal-Water Reaction (W. F. Zelezny)

On the basis of thermodynamic considerations [15] and experimental evidence [16] most of the metals of interest in reactor construction are

capable, in the molten condition, of undergoing explosively violent reactions with water. Attention has been turned to this potential reactor hazard with experiments, both in-pile and out-of-pile, being planned to yield further information on this reaction.

In-pile experiments under consideration include an extension of the work of Elgert and Brown[16] in an attempt to distinguish between the contribution of steam generation and of chemical reaction to the destructive pressure rise produced by the metal-water reaction. Pressure vessels containing $U^{235}O_2$ fuel under water in one series of experiments and Al-$U^{235}O_2$ under water in another series will be exposed to the neutron flux of the MTR. Pressure rises can be due only to steam generation in the first series and to either or both steam generation and chemical reaction in the second series. Because present scheduling commitments for the L-42 position (the only facility in the reactor core that experimental leads can be brought from the reactor) will not make this facility available until well into 1958, and because certain difficulties inherent in reactor testing limit the data program for fiscal 1958 is planned for out-of-pile work. The two phases are to be co-ordinated to supplement each other.

Out-of-pile experiments will include the melting by induction heating of samples of metal under water with attempts to induce violent reactions between this molten metal and the water by the application of (a) ultrasonic waves, and (b) shock waves from the detonation of an explosive cartridge. After success has been attained in the initiation of the metal-water reaction the course of the reaction will be followed by such means as oscillographic pressure recordings and high-speed photography. The objective of this work will be to define more closely the conditions necessary to produce a violent reaction between molten metals and water. With this information as a guide it should be possible to control conditions to prevent or at least reduce the violence of the metal-water reactions.

IV REACTOR PHYSICS AND ENGINEERING

A. Reactor Calculations

1. Reactor Fast Group Constants (D. R. Metcalf)

A method of obtaining the lethargy dependence of the flux $\phi(u)$ from the balance equation,[17]

$$\left[D(u)B^2(u) + \Sigma_a(u)_{SH}(u)\right]\phi(u) = \int_o^u \Sigma_{SH}(u')\phi(u')\, e^{-(u-u')}du' + S(u), \quad \text{IV-1}$$

has been programed for the IBM-650. Cross sections for the individual elements in the SPERT reactors and in the core of the MTR were taken either from BNL-325[8] or its supplement (dated 1957). This program was developed essentially as an aid to obtain the fast group constants for group diffusion theory calculations. The microscopic scattering and absorption cross sections were read at lethargy intervals of 0.1, thus taking quite accurate account of resonance structure. For most elements other than U-235 the absorption cross section was taken as proportional to $\frac{1}{v}$ with a constant σ_a at higher energies such that the resonance integral,

$$\int_{0.4}^{\infty} \sigma_a \frac{dE}{E}, \quad \text{IV-2}$$

would agree with the measured resonance integral values as reported by Pomerance and Macklin at Geneva.[18]

The conventional method of obtaining averaged fast group constants, averaging them over an appropriate flux spectrum, was employed. The low energy cut-off of the fast group was taken to correspond to a lethargy (u) of 18.

B. Fission Product Transient Studies

Previously, preliminary results were given[19] on the yield of I-135 in the fission of plutonium. The data have subsequently been treated further by taking into account burnout of plutonium, the neutron energy dependance of plutonium absorption and fission cross section, isotopic distribution of plutonium, and other factors. The revised result gave a yield of $4.1 \pm 0.6\%$ for I-135. The procedure of making fission product transient measurements and the results obtained on the plutonium napkin ring experiment were prepared for presentation at the second winter meeting of the American Nuclear Society.

C. Thorium Program

A thorium slug irradiated for a year under the RD-1 program (from December 1952 to December 1953) was sectioned and representative pieces analyzed to obtain the distribution of uranium within the slug. No significant angular dependence about the axis of the slug was observed.

The average values as a function of radial distance from the center is summarized in Table 8.

TABLE 8

AVERAGE RADIAL DISTRIBUTION OF URANIUM IN

IRRADIATED THORIUM SLUG

Radial Interval cm.	U-233 Weight %	Isotopic Distribution % of Total Uranium		
		U-233	U-234	U-235
0.0 - 0.5	0.33	98.50	1.45	0.06
0.5 - 0.9	0.34	98.45	1.50	0.05
0.9 - 1.3	0.36	98.26	1.65	0.09
1.3 - 1.55	0.37	98.23	1.65	0.12
1.55 - 1.7	0.40	98.15	1.72	0.14

A depression of about 29% of the surface value is obtained at the center if one assumes the values 0.42 and 0.30 weight percent respectively as the best extrapolated values from the data. This depression compares well with the flux ratios of 26 percent obtained by calculation from simple diffusion theory.

V. NUCLEAR PHYSICS

A. Cross Sections Program (R. G. Fluharty)

The major emphasis of the cross section program has been on understanding the fission process in U-233. Fission cross section data are being studied in terms of the Wigner-Eisenbud multilevel formalism. The 1024 channel analyzer, with strip chart and punch card readouts, has been made an integral part of the fast chopper time-of-flight equipment, replacing the 100 channel analyzer. Data handling procedures which include use of the IBM-650 have been set up. The determinations of resonance parameters from transmission data are continuing.

1. Multilevel Fitting of U-233 Fission Cross Section Data (M. S. Moore, C. W. Reich, L. G. Miller)

Attempts to fit the U-233 fission cross section data from 0.03 to 11 ev are continuing. Crystal spectrometer data are being analyzed by means of a Wigner-Eisenbud multilevel formula[20], which considers neutron capture to be a many channel process. Reasonable fits have been obtained over most of the region being studied.

2. Fission Product Mass Distribution Studies (J. R. Smith, R. B. Regier)

A large fraction of the crystal spectrometer running time has been utilized in making irradiations of U-233 samples at thermal and 1.8 ev energies to study differences in the fission product mass-yield distributions at these two neutron energies. Details of these measurements are described in the chemistry section of this report.

3. Fast Chopper Improvements (F. B. Simpson, O. D. Simpson, C. L. Miller)

For the past six months the 1024 channel analyzer has been operating in parallel with the original 100 channel analyzer. During this period operational debugging, stability improvements, and the development of data handling procedures were in progress. Now the 100 channel analyzer has been removed and the 1024 channel analyzer has been made an integral part of the fast chopper system. The automatic detector delay system and racks to hold amplifiers and power supplies for fission and other special detector systems were installed. A special power distribution system was installed to permit cutting off the power to a section on which work was being done without removing the power from circuits which require extensive warm-up periods for stable operation.

The conceptual design of a shielded automatic sample changer that will be located on the entrance stator of the fast chopper has been completed. Radioactive samples will be transferred pneumatically from a lead transportation pig to the sample changer.

4. The Total Cross Sections of Pu-240 and Gold (O. D. Simpson, R. G. Fluharty)

The total cross sections of Pu-240 and gold, from 0.03 to 42 ev and 0.03 to 1.0 ev, respectively, are shown in Figure 15. The gold cross section was run as a standard and is in good agreement with existing data.

Theoretical fits to the data from the two thinnest samples for the 1.06 ev resonance in Pu-240 are shown in Figure 16. A capture width $\Gamma\gamma = 32 \pm 3$ mv and a neutron scattering width $\Gamma_n = 2.45 \pm 0.15$ mv were determined. These parameters indicate that the 1.06 ev resonance should contribute 317 barns to the thermal cross section. Thermal contributions from the measured levels above 10 ev are less than 3 barns. The difference between this calculated thermal cross section ($\approx$ 320 barns) and the measured value ($\approx$ 390 barns) is not completely understood and is being studied further. The Pu-240 measured cross sections in the higher energy regions appear to be approximately 20 barns too high. The measurements above 42 ev have limited accuracy due to a 20 per cent Pu-239 contaminant and are not shown. Studies are being continued on a limited basis until additional samples, necessary to check these differences, are available.

5. The Total Cross Sections of Neodymium, Samarium, Gadolinium, and Tellurium (F. B. Simpson, R. G. Fluharty)

The total cross sections for neodymium have been computed from the transmission measurements in the energy regions of 0.9 to 12,000 ev. A neodymium oxide sample, which was heated in an oven at 800° C for 16 hours to drive off the water found to be present in previous runs, was used.

The samarium and gadolinium cross section measurements have been extended below 18 ev and the data are presented in Figure 17. The isotopic identifications were made by use of samples enriched in the even-odd isotopes.

The tellurium cross section has been remeasured with a thick sample in order to obtain better values between the resonances. Measurements are being extended to the thermal energy region.

6. The Total Cross Sections of Light Elements (E. H. Magleby, J. R. Smith, L. G. Miller)

Additional measurements of the total cross sections of Ca, Sr, Li-7, Na, and K have been made on both the crystal spectrometer and fast chopper. The data on Ca, Sr, and Li-7 are shown in Figure 18. The Ca data can be considered essentially complete. They indicate a total cross section at thermal energy of 3.08 barns, of which approximately 0.43 barns is due to absorption.

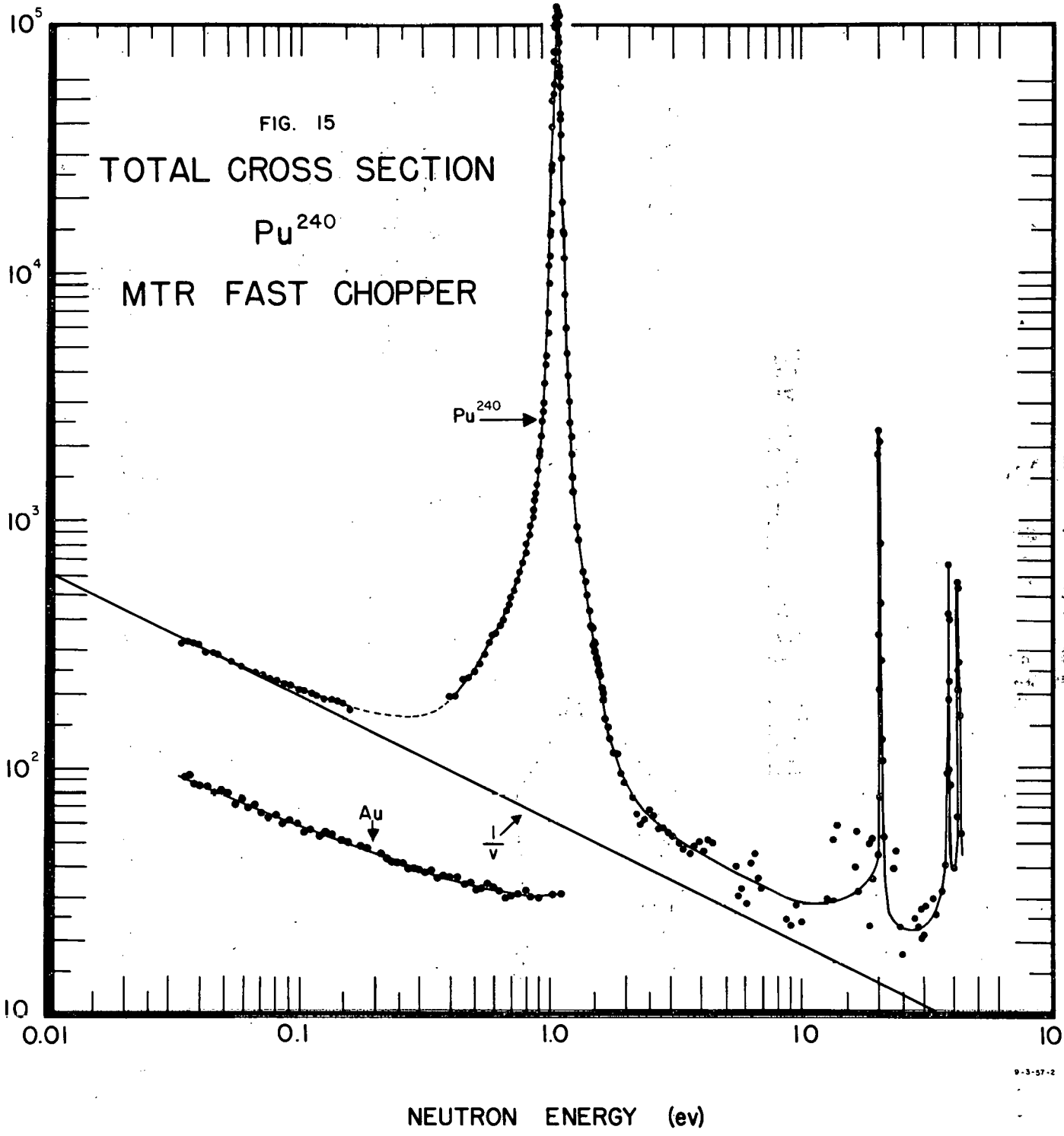
FIG. 15
TOTAL CROSS SECTION
Pu240
MTR FAST CHOPPER
Pu240
Au
1/v
10^5
10^4
10^3
10^2
10
0.01
0.1
1.0
10
100
9-3-57-2
NEUTRON ENERGY (ev)

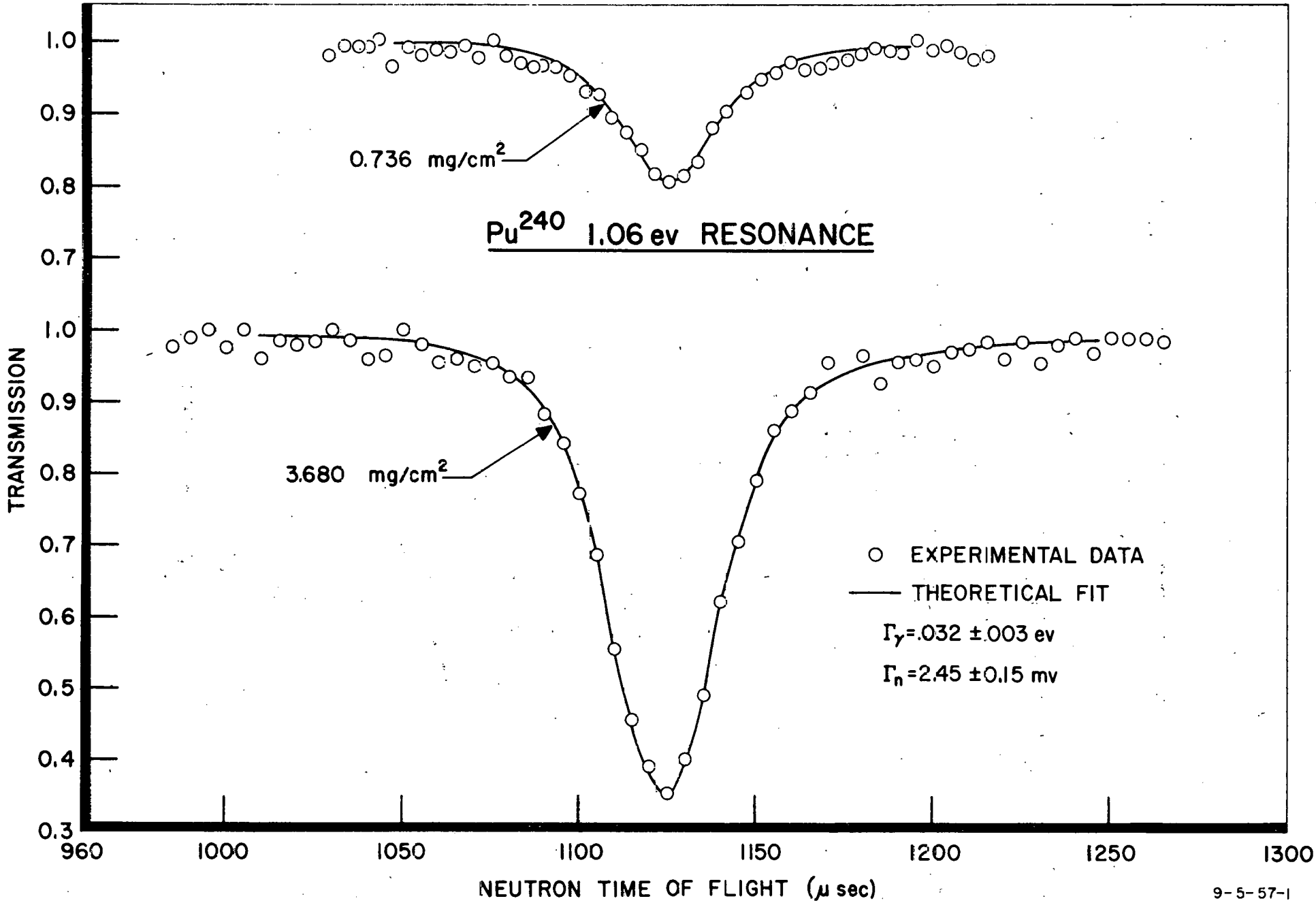
Pu240 1.06 ev RESONANCE
0.736 mg/cm2
3.680 mg/cm2
EXPERIMENTAL DATA
THEORETICAL FIT
Γγ=.032 ±.003 ev
Γn=2.45 ±0.15 mv
TRANSMISSION
NEUTRON TIME OF FLIGHT (μ sec)
1.0
0.9
0.8
0.7
0.6
0.5
0.4
0.3
960
1000
1050
1100
1150
1200
1250
1300
9-5-57-1

FIG. 16

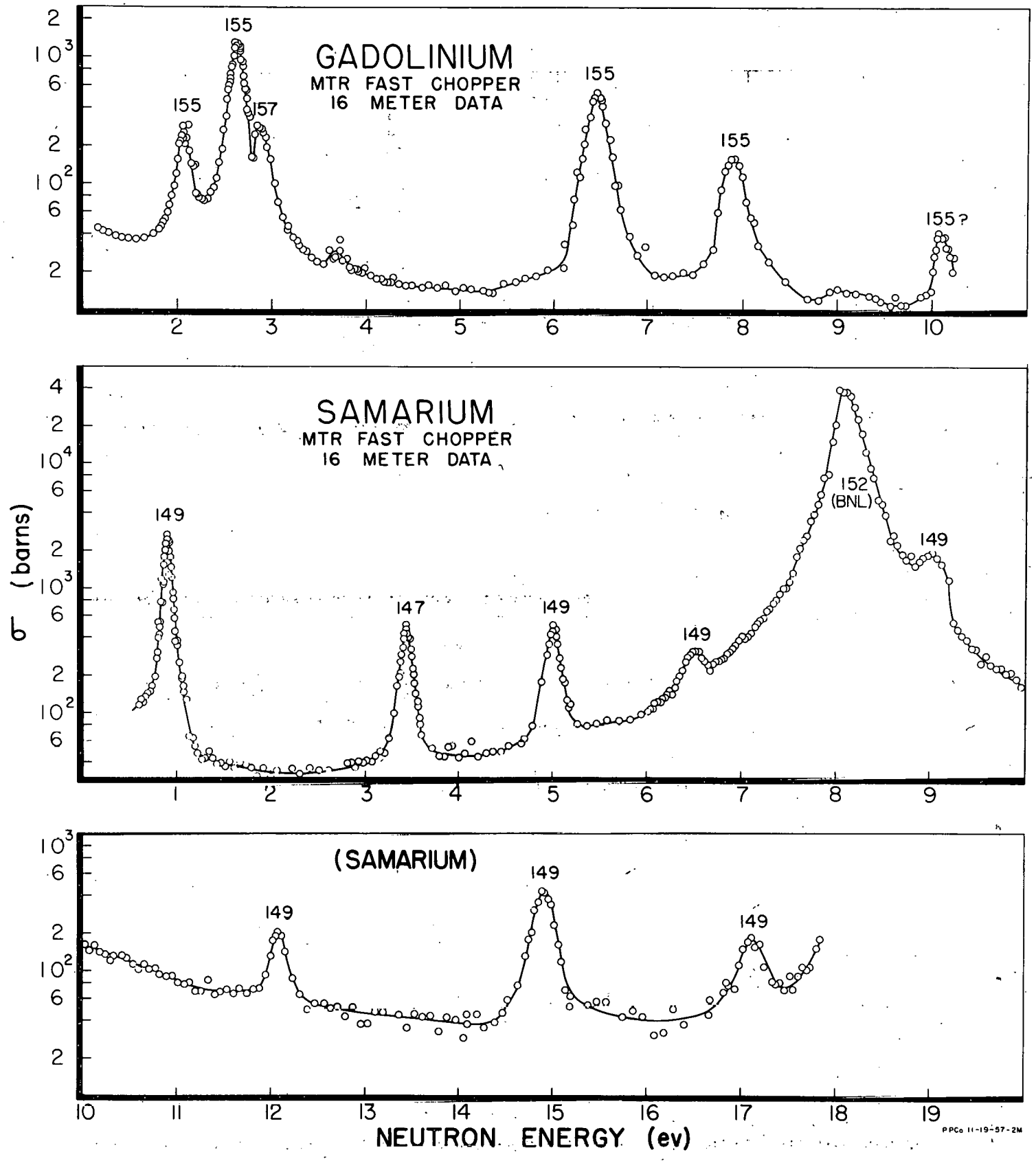
GADOLINIUM
MTR FAST CHOPPER
16 METER DATA
155
155
157
155
155
155?
SAMARIUM
MTR FAST CHOPPER
16 METER DATA
149
147
149
149
152
(BNL)
149
(SAMARIUM)
149
149
149
σ (barns)
NEUTRON ENERGY (ev)
PPCo 11-19-57-2M

FIG. 17

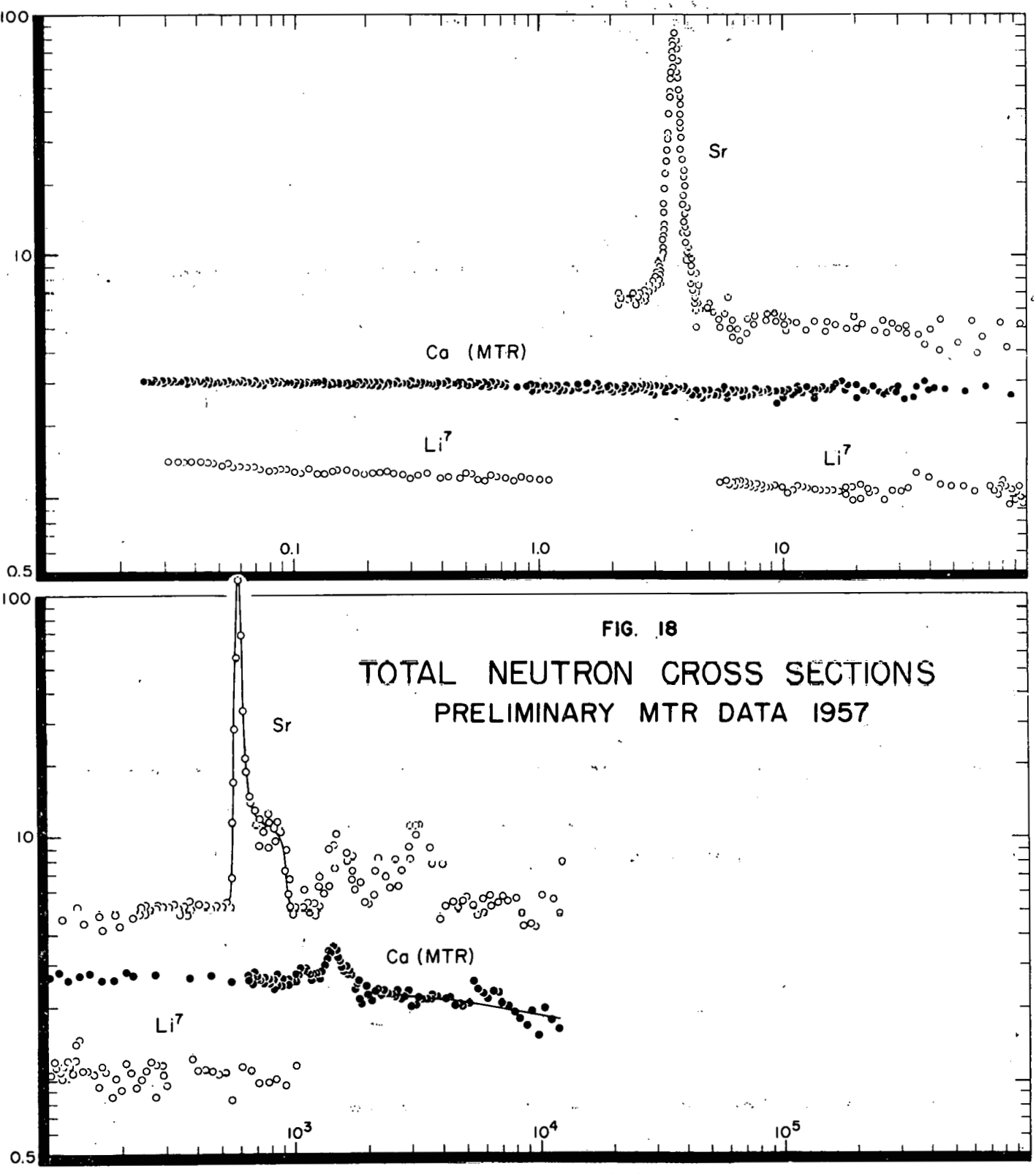

FIG. 18

TOTAL NEUTRON CROSS SECTIONS

PRELIMINARY MTR DATA 1957

B. Inelastic Scattering of Slow Neutrons Program (R. M. Brugger)

1. Experimental Facility Development (R. M. Brugger, L. W. McClellan, J. B. Thompson)

Fabrication of the HG-6 beam hole plug has been completed and the plug has been installed in the MTR. The plug has an internal nickel steel gate which also serves as a variable width (from 0 to 2") collimator. The maximum beam size is 4 inches in height by 2 inches in width. For an MTR operating power of 40 Mw, thermocouples attached to the tip of the collimator plug gave a temperature reading of 54° C when the plug was evacuated and 48° C when the plug was air filled.

Radiation level measurements have been made around the catcher tanks with the full 2" x 4" beam open to the catcher. The slow and fast neutron levels are reduced below biological tolerances by the catcher, but the gamma-ray level is 45 mr/hr in the beam beyond the catcher. This beam has penetrated 2" LiF, 15" borated paraffin, 4" lead and 5' water. An additional 4" of lead will be added to further reduce the gamma-ray level.

The duranickel "R" for the chopper rotors has been delivered. Three bids have been received for machining and heat treating these rotors.

Three phase 4-pole synchronous motors have been ordered to drive the phased rotors. They will operate from 300 to 30,000 rpm and will be powered by a variable frequency oscillator and three 200 watt amplifiers.

The detailed drawings for the rotor chambers and adjustable mounts are essentially complete and construction should be completed by approximately January 1, 1958.

2. 1024 Channel Analyzer for Velocity Selector (F. L. Petree)

Initial development has begun of a 1024 channel time-of-flight analyzer. It will be similar to the unit which was recently completed for the MTR fast chopper, in that it will utilize a matrix of ferrite magnetic memory cores to store the data as they accumulate.

It is planned that this device will utilize transistors as amplifying and current-generating elements. It will employ a temporary-storage matrix of 100 ferrite cores. This will reduce the effective dead-time to less than two micro-seconds, by temporarily storing the random detector pulses so that they can be presented to the permanent-storage matrix at regular intervals. Besides reducing the dead-time, this feature will allow memory cores with less stringent drive requirements to be used in the permant-storage matrix, so that direct drive from transistor current generators will be feasible. The memory matrix can be divided so that separate storage from as many as sixteen detectors will be possible. It will require twenty microseconds to store a pulse into the permanent-storage matrix, so that the maximum permissible counting rate will be less than 50,000 per second. At this rate, the counting loss will be less than ten per cent if the temporary-storage matrix does not fill up.

The channel width of this instrument will be adjustable by factors of two from 2.5 to 160 microseconds. An adjustable initial delay up to a maximum of 10,240 microseconds will be provided.

The instrument will continuously display the stored information on a cathode ray oscillograph. Data readout onto a strip-chart recorder and into punch-cards will be provided.

C. Nuclear Chemistry Program (W. H. Burgus)

1. Mass Yields in the Resonance Fission of U-233 (R. B. Regier, W. H. Burgus)

Measurements are being made to determine if there are differences in the peak-to-trough ratios of fission product mass-yield curves of U-233 for fissions produced by thermal neutrons and for those produced by 1.8 ev neutrons. It is expected that the relative amounts of symmetric and asymmetric fission depend on the spin state of the compound nucleus. Also the multilevel fitting experience[20] of MTR Cross Section personnel indicate that most thermal fissions in U-233 are due to one spin state while the fissions produced by neutrons at many of the resonance energies are due to the other spin state. Since fission products having yields lying in the trough of the mass yield curve are from nearly symmetric fission and those on the peaks are from asymmetric fission, the observed saturation activity ratios between properly selected fission products near one of the peaks and in the trough will indicate the ratios of symmetric and asymmetric fission.

In the first experiments the ratios of the saturated activity of 67 h Mo-99 (near top of light peak) to the saturated activity of 5.3 h Ag-113 (in the "trough") were compared for thermal neutron fission and for fission with 1.8 ev neutrons, the energy of the first large resonance in U-233 fission. For the thermal irradiations, small milligram size samples of U-233 were irradiated in VG-23 of the MTR. The Mo^{99}/Ag^{113} saturation activity ratios observed in several runs averaged 394 with an estimated accuracy of 5 percent. (Subsequent experiments in which Mo^{99}/Ag^{111} ratios were compared for VG-23 irradiations and for irradiations in the thermal beam of the MTR crystal spectrometer have indicated no significant difference in the ratios between the two thermal irradiations.) In the thermal irradiations in position VG-23 in the reactor there was ample flux to produce fission product samples having counting rates in the range of thousands of counts per minute, even when irradiating small quantities of U-233. This was not true, however, in the spectrometer runs where only small yields of fission products were obtained due to much lower flux.

For irradiations on the crystal spectrometer at 1.8 ev, larger (2 to 3 grams) portions of U-233 oxide were required to obtain measurable 5.3 h Ag-113 activity. The use of larger samples, however, introduced a new problem; that of isolating and purifying the low-activity fission product samples from the several millicuries of alpha, beta, and gamma activities present in the original uranium oxide. The standard fission product isolation procedures were found to yield samples still contaminated with the decay products of U-233 and U-232, and improved methods of fission product analyses had to be devised.

Four irradiations of 2-3 gram portions of U-233 oxide were carried out with 1.8 ev neutrons in the Bragg beam of the MTR crystal spectrometer using the $(10\bar{1}1)$ planes of a beryllium crystal for diffraction. The estimated energy resolution was 15 percent. Each irradiation was of 18 hours duration so that near-saturated 5.3 h Ag-113 was obtained. The saturated Ag-113 activity for these irradiations was of the order of 300 counts per minute at 100 percent chemical recovery. However, the chemistry required approximately one half-life of Ag-113 and recovery was only about 50 percent in the four samples. For resolution of the silver decay curves, each sample was counted at about half hour intervals during the first 20 hours to resolve the Ag-112 and Ag-113 components then at longer intervals to obtain the Ag-111 activity. The Ag-113 activity at the end of 20 hours was therefore only several counts per minute above background. The Mo^{99}/Ag^{113} ratios for these resonance irradiations were 469, 471, 485, and 567 for an average of 498 with a standard deviation of $\pm$ 47. The data indicated that the "peak-to-trough" ratio for resonance fission (498) is greater by about 25 percent than for thermal fission (392). The lack of precision in the spectrometer experiments is discomforting and is believed partially due to the difficulty of resolving the silver decay curve into its 3.2 h Ag-112, 5.3 h Ag-113 and 7.5 d Ag-111 components, particularly with low counting samples. The values for Ag-113 used in computing the above ratios were obtained from a least-squares analysis of the counting data, assuming pure silver samples.

Additional work is underway to examine changes in "peak-to-trough" ratios using Mo-99, Ag-111 and Cd-115. A low background counting system is being assembled to improve the statistical accuracy.

2. Second Order Capture Measurements (R. B. Regier, E. H. Turk, R. P. Schuman)

Specimens of natural potassium, antimony, rhodium, and enriched Ru-104 were irradiated in position L-45 in the MTR during Cycle 90, at a flux of 5.4×10^{14} $n/cm^2/sec$, in attempts to measure the pile cross section of K-42, Sb-124, Rh-104, and Ru-105. The antimony and ruthenium will be allowed to decay until about mid 1958 before they are examined.

All attempts to detect Rh-105 by gamma spectroscopy were unsuccessful. The rhodium was processed by ion exchange chemistry, following the procedure outlined in Analytical Chemistry.[21] This procedure failed to remove all the iridium impurity (20 ppm according to the supplier) and the Ir-192 completely masked any Rh-105 that may have been formed.

Samples of spectroscopically pure magnesium, nickel, and chromium were irradiated in VH-2 facility of the MTR ($nv = 1.87 \times 10^{14}$ $n/cm^2/sec$) for $\approx$ 18 hours to study the production of the second order neutron capture nuclides (Mg-28, Ni-66, Cr-56). After irradiation the samples were chemically purified and the activities present determined by scintillation spectrometry and beta proportional counting.

The magnesium sample was purified by dissolution in hydrochloric acid, followed by repeated precipitations of magnesium hydroxide, and repeated scavenging precipitations of ferric hydroxide, ferrous sulfide and

manganese sulfide from ammoniacal solutions. The magnesium was finally precipitated as magnesium ammonium phosphate for counting. Very little activity was found in the final purified precipitate, which was counted ≈ 1 day after the end of bombardment. From the known half-life of Mg-28 (21.4 hrs) and the maximum possible 32 kev gamma activity observed (corrected for absorption) a pile neutron capture cross section of ≤ 20 mb for Mg-27 was calculated.

The nickel sample was dissolved in hydrochloric acid, and purified by repeated precipitations as nickel dimethylglyoxime and ferric hydroxide scavenging precipitations. The nickel was finally precipitated as the sulfide for counting. The activity of the Cu-66 daughter formed by beta decay of Ni-66 was studied by two different methods: (1) by beta proportional counting with an aluminum filter; and (2) by pulse height analysis of the 1.044 Mev gamma photopeak with the scintillation spectrometer. The decay of the beta and gamma activities were observed and gave for the half-life of Ni-66 ≈ 54 hours, compared to 55 hours given by W. H. Sullivan.[22] The sample contained a considerable amount of 36 h Ni-57 produced by the (n, 2n) reaction on Ni-58. The disintegration rate of the Ni-66 calculated from the scintillation counting, assuming a 9 per cent branching ratio for the 1.044 Mev Cu-66 gamma, and the rate calculated from beta counting the Cu-66 2.63 Mev + 1.59 Mev betas agreed within 6 per cent. A pile neutron capture cross section of 20 barns was obtained for Ni-65 in the MTR VH-2 facility.

An attempt was made to obtain Cr-56 by second order neutron capture in Cr-54. As a method of analyzing for Cr-56, manganese was separated, then the regrowth of Mn-56 into the purified chromium was sought. No growth of Mn-56 could be observed, indicating little or no production of Cr-56.

3. Study of (t,p) Reactions (E. H. Turk, R. P. Schuman)

In order to study another method of production of nuclides with two more neutrons than the target nucleus, the (t,p) reaction products produced by thermal neutron irradiations of a mixture of the target nucleus and enriched Li-6 were investigated. The tritons are made by the reaction Li-6 (n,α) H-3 and have 2.7 Mev of kinetic energy.

Irradiations were made of mixtures of MgO, Ni, Cr, and $U_3^{238}O_8$ with $Li_2^6SO_4$. A good yield of Mg-28 was obtained. In the cases of Ni and U, the yield was no greater than that produced by the second order neutron capture reactions. No evidence was found for Cr-56.

4. Studies of Short-lived Fission Products (E. H. Turk, R. P. Schuman)

Samples of enriched uranium were activated in the VG facilities of the MTR for short periods (1-5 min). The fission product zirconium sample was isolated (≈ 6 min after end of irradiation) using barium fluozirconate precipitations with lathanum fluoride scavenging precipitations. No new fission product zirconium activities are formed with appreciable yields and with half-lives greater than 2 minutes.

Short-lived barium fission products were also isolated from samples of enriched uranium irradiated for short periods (1-5 min) in the VG facilities of the MTR. The barium was isolated and purified as rapidly as possible (≈ 6 min after end of irradiation) by repeated barium chloride precipitations and ferric hydroxide scavengings. The decay of the various gammas in the purified samples was studied with a 20-channel scintillation spectrometer. The energies and approximate half-lives found are given in Table 9. The gamma activities with 11 minute half-lives are believed to be due to Ba-142. This is in disagreement with the value of 6 minutes which has been used [22] for the half-life of Ba-142 for some time.

TABLE 9

Gamma Energies and Half-Lives

Found in Short-Lived Barium Fission Products Studies

(kev)	T-1/2 (min)	Chemical Identification of Activity
70	11	Ba
180	18	Ba
260	17	Ba
460	18	Ba
640	83	La-142
740	(?)	(?)
900	12	Ba
900	83	La-142
1060	14	Ba
1200	12	Ba
1380	12	Ba & La-142 (?)
1640	10	Ba

5. Xenon Gas Purification (S. D. Reeder)

A sample of fission product xenon obtained from the Chemical Processing Plant is being purified for cross section measurements on the MTR fast chopper and for other studies. The sample contained 19% xenon and O_2, N_2, N_2O, and Kr impurities. Some purification was achieved when the sample was transferred to a lecture size cylinder from the 1A size gas cylinder in which it was delivered. The transfer was made by freezing the gas at a pressure of about 3 cm of Hg in a trap cooled in liquid nitrogen. Some oxygen, nitrogen and most of the krypton were pumped off in this step. The solidified gases were then distilled into the evacuated lecture cylinder cooled in liquid nitrogen. The higher boiling oxides of nitrogen were allowed to escape after all of the xenon was believed to be transferred.

A mass analysis of the collected gas gave the following composition: 26% Xe, 46% N_2, 12% O_2, and 15% N_2O. The xenon will be separated from the other gases by passing the mixture over hot calcium and titanium metals which convert the impurities to solid oxides and nitrides.

D. Decay Schemes and Nuclear Isomerism Program

1. Experimental Check of Calculated Scintillation Detector Efficiencies (S. H. Vegors, R. L. Heath)

A program has been initiated to make an evaluation of the accuracy of machine calculated detection efficiencies for NaI(Tl) scintillation detectors. The major error to be expected in the calculated values may be attributed to errors in the experimentally determined values for the absorption cross section of NaI(Tl). It was felt that a check of the internal consistency of the machine program could be obtained by measuring several monoergic sources under known geometrical conditions using different size detectors. Since the probability for interaction in the phosphor is proportional to the product of absorption cross section and the path length traversed by the photon, a measurement of the number of photons detected by different size detectors should provide an independent check on the error in the absorption cross section.

Three sources were measured on each of two different sizes of NaI(Tl) detectors (1 3/4" dia. x 2" and 3" dia. x 3" cylinders) and the source intensity calculated for each case. The results are shown in Table 10. It is felt that the small discrepancies in the values for the disintegration rates represent the accumulative effects of errors in the experimental method. These measurements were made using a source-detector distance of 3.00 ± 0.05 cm for the 1 3/4" detector and 10.00 ± 0.05 cm for the 3" x 3" detector.

TABLE 10

Comparison of the Disintegration Rates of Several Sources as Measured by Two Different Detectors

Radioactive Source	Gamma Ray Energy (kev)	1 3/4" dia. x 2" Thick	3" dia. x 3" Thick	Percent Difference
Zn-65	1114	57,163	59,660	4.2
Cs-137	662	25,641	25,727	0.3
Cr-51	323	25,544	24,677	3.4

2. Scintillation Detector Calculations (S. H. Vegors, R. L. Heath)

Calculations of the detection efficiency of a right cylindrical NaI(Tl) scintillation detector for gamma rays emitted by a disk source of radiation are near completion. The investigation of the detection efficiency for non-point sources of radiation will be extended to cover the case of a line source of radiation. A code is being prepared by the computer group to permit computation on the IBM-650 for a line source of radiation. Calculations for this case should begin in the immediate future. The results of these calculations will be included in tabular form in an IDO report.

3. Finite Solid Angle Correction For Angular Correlation Studies (S. H. Vegors)

Since the detector used in angular correlation measurements subtends a non-zero solid angle with the source of radiation it is necessary to make a correction to the experimental data to take this into account. An analytical expression for this correction factor has been given by Rose.(23) No calculations have previously been made, however, to yield this correction factor for the detector sizes and distances which are to be used in the angular correlation device being constructed at this laboratory. Therefore, a code has been prepared by the computer group to calculate this effect and calculations have been made for a 3" dia. x 3" thick NaI(Tl) crystal for a source-detector distance of 10 cm. These results are listed in Table 11. The notation used in the table is identical with that of Rose.(23)

4. Photo-Peak Efficiencies (Peak-To-Total Ratios) For NaI(Tl) Detectors (S. H. Vegors, W. M. Hammer, R. L. Heath)

As a part of the program to increase the precision and usefulness of absolute gamma-ray counting, using the scintillation spectrometer as a quantitative and qualitative tool for radioactivity analysis, measurements have been made of the peak-to-total ratio for a 1 3/4" dia. x 2" dia. NaI(Tl) crystal.

To minimize the error due to extraneous scattered radiation from material in the vicinity of the detector the measurements were all made in an open room with all scattering material removed from the immediate vicinity. Point sources were mounted on thin films and measurements were made at source detector distances of 3 cm and also at 10 cm for several sources. In most cases no beta absorber was necessary since electron-capture activities were used. For some energy regions it was necessary, however, to use low energy beta emitters necessitating the insertion of polystyrene absorbers. Measurements were made at the following energies: 0.155 (Sc-47), 0.323 (Cr-51), 0.478 (Be-7), 0.662 (Cs-137), 0.835 (Mn-54), 1.114 (Zn-65), 1.368 (Na-24), 2.753 (Na-24), and 3.13 Mev (S-37). A summary of the results is given in Table 12. The error quoted is an estimate taking into consideration the experimental uncertainties in each case.

5. Decay of 14.5 Day Bi-205 (S. H. Vegors and R. L. Heath)

A new source of Bi-205 has been procured and the investigation of the decay of Bi-205 is continuing using the new source. This source was prepared by bombarding radiogenic lead which is approximately 85% Pb-206 for 10 hours in the proton beam of the ORNL cyclotron. The source thickness and bombardment energies were picked to maximize the production of Bi-205 relative to Bi-206 (6.4 day) or Bi-207 (8.0 year) by a Pb-206 (p,2n) Bi-205 reaction. The new source is much freer of the 8 year Bi-207 activity and thus the investigation of the decay scheme of Bi-205 is considerably simplified. In both the new source and the previous source the 6.4 day Bi-206 activity was allowed to decay away before measurements were begun. Preliminary investigations with the new source indicate that it will be much more satisfactory than the previous source. Remeasurement of gamma-ray energies, relative intensities, and coincidence relationships is now in progress.

TABLE 11

Attenuation coefficients J_ℓ/J_o and $(J_\ell/J_o)^2$ for angular distribution measurements. These values are for 3" diameter x 3" thick NaI(Tl) detectors with the distance from the source to the front face of the detector being 10 cm (for values of ℓ = 0, 2, and 4).

(cm^{-1})	J_o	J_2	J_4	J_2/J_o	$(J_2/J_o)^2$	J_4/J_o	$(J_4/J_o)^2$
.127	.01322	.01232	.01040	.93221	.86902	.78670	.61890
.130	.01342	.01251	.01056	.93211	.86883	.78638	.61839
.150	.01471	.01371	.01154	.93142	.86754	.78432	.61516
.200	.01738	.01616	.01355	.92976	.86445	.77936	.60740
.300	.02101	.01948	.01619	.92677	.85890	.77041	.59353
.500	.02480	.02287	.01876	.92205	.85018	.75635	.57207
.700	.02668	.02451	.01992	.91872	.84405	.74652	.55729
1.000	.02823	.02584	.02080	.91544	.83803	.73683	.54292
2.000	.03030	.02759	.02189	.91047	.82896	.72234	.52178
3.000	.03109	.02824	.02227	.90844	.82526	.71648	.51334
5.000	.03177	.02880	.02260	.90662	.82196	.71125	.50588
7.000	.03209	.02906	.02274	.90576	.82040	.70878	.50237
10.000	.03234	.02927	.02286	.90506	.81913	.70678	.49954
20.000	.03265	.02952	.02300	.90420	.81758	.70434	.49609
40.000	.03275	.02961	.02304	.90391	.81705	.70351	.49493
70.000	.03276	.02961	.02305	.90388	.81700	.70343	.49481
100.000	.03276	.02961	.02305	.90388	.81700	.70343	.49481

TABLE 12

Summary of Peak-To-Total Ratios for a 1 3/4" dia. x 2" NaI(Tl) Crystal

Radioactive Isotope	Gamma Ray Energy In Mev	P/T (Source 3 cm)	P/T (Source 10 cm)
Sc^{47}	.155	.95 ± .02	
Cr^{51}	.323	.72 ± .03	.72 ± .03
Be^{7}	.478	.54 ± .02	
Cs^{137}	.662	.39 ± .02	.39 ± .01
Mn^{54}	.835	.337 ± .01	
Zn^{65}	1.114	.273 ± .01	
Na^{24}	1.368	.248 ± .01	.240 ± .01
Na^{24}	2.753	.130 ± .005	.128 ± .005
S^{37}	3.13	.104 ± .004	.106 ± .004

6. Decay of La-142 (R. L. Heath and L. D. McIsaac*)

The decay of this nuclide was first established by Hahn and Strassmann [24] in 1942. In their work a lanthanum activity with a half-life of 77 minutes was assigned to La-142 by chemical isolation from the 6 minute half life Ba-142 activity in gross fission products. Katcoff [25] also reports this activity in project literature. Bosch [26] studied the lanthanum fraction of gross fission products in further detail and reported two major gamma rays of 0.63 and 0.89 Mev. No further details of the decay of this nuclide have been reported in the literature.

Some further work has been done on this activity at this laboratory in conjunction with the preparation of standard spectra for scintillation spectrometry.[27]

a. Sample Preparation

Samples of enriched uranium were activated in a high flux facility of the MTR for 30 seconds and after a waiting period of approximately 5 minutes the barium chemical fraction was separated from gross fission products. The 6 minute Ba-142 precursor was then allowed to decay for 10 minutes and a lanthanum chemical fraction separated from the barium. This procedure provided samples of Lanthanum-142 relatively free of other activities.

b. Gamma Radiation

The gamma radiation emitted was investigated with the 100-channel gamma-ray spectrometer using a 3-inch by 3-inch NaI detector. The pulse spectrum obtained indicated a large number of gamma-rays which decayed with a half-life of 88 ± 5 minutes. The following energies were assigned to the major gamma-rays: 0.645, 0.89, 1.03, 1.37, 1.54, 1.72, 1.91, 2.05, 2.4, 2.55, 2.95, and 3.1 Mev. A characteristic pulse spectrum is shown in Figure 19.

---

* Westinghouse Atomic Power Division employee assigned to sponsors program at MTR.

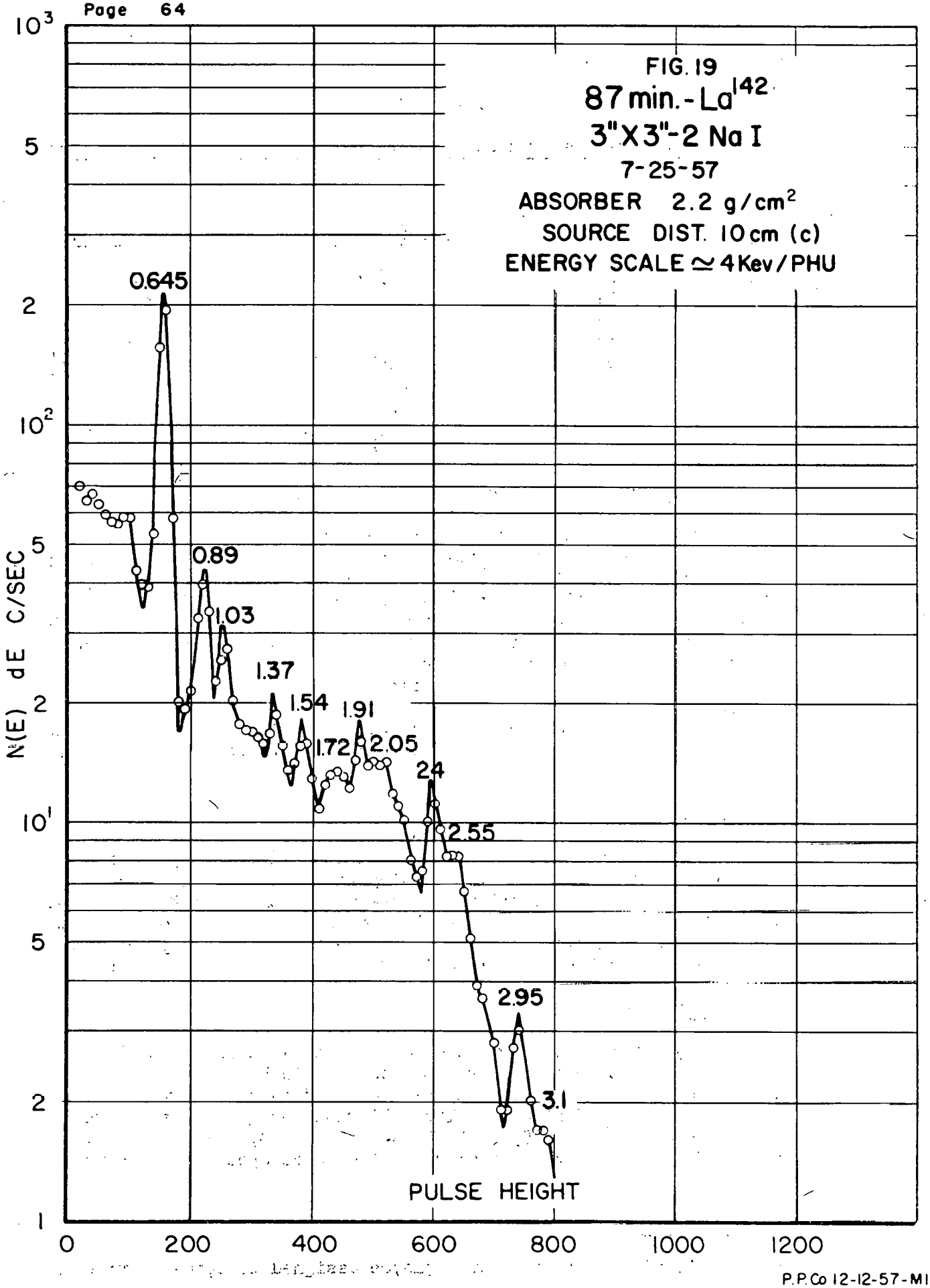

P.P.Co 12-12-57-MI

c. Beta-Ray Measurements

A sample was prepared for beta counting on a calibrated end-window flow proportional counter and the decay rate followed for a period of 24 hours. The decay curve obtained indicated the presence of two activities with half-lives of 85 minutes and 3.9 hours. These were assigned to 88 minute La-142 and 3.8 hour La-141. A comparison of the La-142 activity of this sample with the emission rate for the 0.645 Mev gamma-ray as measured on the scintillation spectrometer indicated that 50 + 10% of the beta transitions give rise to the 0.645 Mev gamma-ray. Additional measurements are planned to obtain more detailed information on the nature of the decay of this nuclide.

VI. PAPERS AND PUBLICATIONS

A. IDO Reports Issued

IDO No.	Title	Authors
16334	Reactor Charge Life with Burnable Poisons	H. L. McMurry
16335	Reactivity Excursions in the ETR	H. L. McMurry
16373	MTR Technical Branch Quarterly Report First Quarter, 1957	Editor: W. B. Lewis
16378	Plutonium Fuel Requirements for Operation of the MTR	H. L. McMurry B. W. Johnson
16379	Calculation of ETR Charge Life Using ETR Critical Facility Data	H. L. McMurry P. W. Healy
16384	Comparison of Flux and Power Distributions, and Void and Temperature Coefficients of the MTR with U-235 and Pu-239 Fuel	B. W. Johnson H. L. McMurry
16389	A Neutron Absorption Alignment Chart	R. G. Nisle
16390	A Four Region, Two Group Calculation of SPERT-III Critical Size and Flux Distribution	D. R. Metcalf V. C. Kobold
16391	Relative Neutron Lifetimes in the MTR Fueled with U-235 and Pu-239	H. L. McMurry B. W. Johnson
16394	Quarterly Progress Report for MTR Technical Branches - Second Quarter, 1957	Editor: J. E. Evans
16398	Reactivity Effects of Xe-135 and Sm-149 for the MTR with U-235 and Pu-239 Fuels	B. W. Johnson H. L. McMurry
16399	Debye Characteristic Temperatures Table and Bibliography	M. W. Holm

B. Papers Presented at Meetings

1. Papers Presented at the International Conference on Neutron Interactions with Nuclei at Columbia University, New York City, New York, September 9-13, 1957.

   a. J. E. Evans, Neutron Interactions with U-233 for Neutron Energies $\leq 10^4$ ev.

Papers Presented at Meetings - contd.

b. R. G. Fluharty, Recent Neutron Total Cross Section Measurements.

2. Paper Presented at the ANP Spectroscopy Information Meeting in Dayton, Ohio, August 4-7, 1957.

a. R. L. Heath, Standardization of Techniques on the Use of Scintillation Spectrometry for Routine Analysis.

3. Paper Presented at the Annual Materials Control Conference in Washington, D. C., June 17-20-, 1957.

a. F. P. Vance and F. H. Tingey, Nucleonic Assay of Reactor Fuel.

VII. REFERENCES

(1) J. E. Evans, Quarterly Progress Report for MTR Technical Branches, IDO 16394: (p. 7) August 22, 1957.

(2) W. C. Francis and L. L. Marsden, Experimental and Theoretical Values of the Gamma Decay Dose Rate and Heating from Spent MTR Fuel Elements, IDO 16247: January 13, 1956.

(3) J. E. Evans, ibid., (p. 10).

(4) J. E. Evans, ibid., (p. 20).

(5) H. L. McMurry, Estimation of Fuel Requirements for Two Weeks Operating Cycles in the MTR, IDO-16140: December 2, 1953.

(6) H. L. McMurry, G. A. Cazier, and R. W. Goin, Calculation of MTR Fuel Charges, IDO 16401: September 27, 1957.

(7) H. L. McMurry and G. A. Cazier, Extrapolated Charge Life from Ingrowth of Xe-135, IDO 16413: October 2, 1957.

(8) D. J. Hughes and J. A. Harvey, Neutron Cross Sections, BNL 325: 1955.

(9) B. Wolfe, Final Physics Report for the Engineering Test Reactor, Vol. 1 (Report prepared by Atomic Power Equipment Department, General Electric Co., for Kaiser Engineers Division of Henry J. Kaiser Co., for Idaho Operations Office, U. S. Atomic Energy Commission, Idaho Falls, Idaho), June 25, 1956.

(10) J. W. Webster, Reactivity Effect of Reducing the Al/H_2O Ratio In The MTR Core, IDO 16133: October 26, 1953.

(11) J. E. Evans, ibid., (p. 31).

(12) J. H. Perry, Editor-in-Chief, Chemical Engineers Handbook, Third Edition, McGraw-Hill Book Company.

(13) R. J. Nertney, Calculated Surface Temperatures for Nuclear Systems and Analysis of Their Uncertainties, IDO 16343: June 1, 1957.

(14) J. E. Evans, ibid., (p. 34)

(15) W. C. Ruebsamen, F. J. Shon, J. B. Chrisney, Chemical Reaction between Water and Rapidly Heated Metals, TID 10056: October 27, 1952.

(16) O. J. Elgert and A. W. Brown, In-Pile Molten Metal-Water Reaction Experiments, IDO 16257: June 30, 1956.

(17) A. L. Boch, W. R. Gall, G. F. Leichsenring, R. S. Livingston, A Conceptual Design of a Pressurized Water Power Packaged Reactor, ORNL 1613, June 6, 1955.

(18) R. L. Macklin and H. S. Pomerance, Resonance Capture Integrals, A/Conf. 8/P/833: July 18, 1955.

(19) J. E. Evans, ibid., (p. 44).

(20) J. E. Evans, ibid., (p. 48).

(21) W. M. MacNevin and E. S. McKay, Separation of Rhodium, Palladium, and Iridium by Ion Exchange, Analytical Chemistry, 29, 1222 (1957).

(22) W. H. Sullivan, Trilinear Chart of the Nuclides, 1957.

(23) M. E. Rose, The Analysis of Angular Correlation and Angular Distribution.

(24) O. Hahn and F. Strassmann, Naturwiss. 30, 324 (1942).

(25) S. Katcoff, NNES-PPR 9, 1147 (1951).

(26) A. V. Bosch, Physica 19, 374 (1953).

(27) R. L. Heath, Scintillation Spectrometry Gamma-Ray Spectrum Catalogue, IDO 16408, July 3, 1957.

PREVIOUS QUARTERLY REPORTS IN THIS SERIES

IDO 16291	First Quarter 1956
IDO 16297	Second Quarter 1956
IDO 16314	Third Quarter 1956
IDO 16331	Fourth Quarter 1956
IDO 16373	First Quarter 1957
IDO 16394	Second Quarter 1957


Phillips
66